

Geodesics of the Schwarzschild Black Hole with String Cloud Background

by

Mahwish Batool



Supervised by

Dr. Ibrar Hussain

Submitted in the partial fulfillment of the

Degree of Master of Philosophy

in

Mathematics

School of Natural Sciences

National University of Sciences and Technology

Islamabad, Pakistan.

February 2016


National University of Sciences & Technology

M.Phil THESIS WORK

We hereby recommend that the dissertation prepared under our supervision by: Mahwish Batool, Regn No. NUST201361932MSNS78013F Titled: Geodesics of Schwarzschild black hole in string cloud background be accepted in partial fulfillment of the requirements for the award of M.Phil degree.

Examination Committee Members

1. Name: DR. MUBASHER JAMIL

Signature: 

2. Name: DR. RIAZ AHMAD KHAN

Signature: 

3. Name: DR. SAJID ALI

Signature: 

4. Name: DR. MANSOOR UR REHMAN

Signature: 

Supervisor's Name: DR. IBRAR HUSSAIN


Signature: 


Head of Department

03-03-2016
Date

COUNTERSIGNED

Date: 03/03/16


Dean/Principal

Abstract

In this thesis the trajectories of the timelike and null geodesics for radial and circular motion of Schwarzschild black hole with string cloud background are investigated and compared with Schwarzschild case without string clouds. It is found that in the presence of string cloud parameter the horizon is larger than the Schwarzschild horizon. Effective potential is calculated, it is observed that the effective potential decreases for the increasing value of string cloud parameter. It is also found that for larger value of string cloud parameter the circular orbit of photon has larger radius and vice versa. Hence, as the value of string cloud parameter increases the particle can more easily escape to infinity. Stability of circular orbits is also discussed.

Acknowledgements

All praise to Almighty Allah, Who showered His endless blessings on me and for giving me strength to carry out my work successfully. My deepest gratitude to my supervisor Dr. Ibrar Hussain for providing guidance and constructive comments that has contributed greatly to the success of this research. This thesis would not have been possible without his supervision and persistent help. I would like to thank him for giving me an opportunity to work with him on an interesting topic. Special thanks to my GEC members Dr. Mubasher Jamil (SNS), Dr. Sajid Ali (SEECS) and Dr. Riaz Ahmad Khan (SMME). In the end, I would also like to thank my family especially my parents for their unconditional support and encouragement.

Contents

| | | |
|----------|--|----------|
| 1 | Introduction | 7 |
| 1.1 | Metric Tensor | 11 |
| 1.2 | Geodesics | 12 |
| 1.3 | Riemann Tensor and Other Related Tensors | 13 |
| 1.4 | Einstein Tensor | 15 |
| 1.5 | Stress-Energy-Momentum Tensor | 15 |
| 1.6 | Derivation of Einstein Field Equations for Vacuum | 16 |
| 1.7 | The Einstein Field Equations in the Presence of Matter | 19 |
| 1.8 | Black Holes | 20 |
| 1.9 | Singularity | 22 |
| 1.10 | Event Horizon | 23 |

| | | |
|----------|---|-----------|
| 2 | Rindler Modified Schwarzschild Geodesics | 24 |
| 2.1 | Particle Trajectories | 26 |
| 2.2 | Radial Motion | 28 |
| 2.2.1 | Null Geodesics | 29 |
| 2.2.2 | Timelike Geodesics | 29 |
| 2.3 | Circular Motion | 32 |
| 2.3.1 | Null Geodesics | 34 |
| 2.3.2 | Timelike Geodesics | 38 |
| | | |
| 3 | Motion of a Particle in the Spacetime Field of the Schwarzschild Black Hole with String Cloud Background | 42 |
| 3.1 | Introduction | 42 |
| 3.2 | Particle Trajectories | 48 |
| 3.3 | Radial Motion | 50 |
| 3.3.1 | Null Geodesics | 50 |
| 3.3.2 | Timelike Geodesics | 51 |
| 3.4 | Circular Motion | 56 |

| | | |
|----------|-------------------------------|-----------|
| 3.4.1 | Null Geodesics | 58 |
| 3.4.2 | Timelike Geodesics | 61 |
| 4 | Summary and Discussion | 68 |
| 5 | Bibliography | 69 |

Chapter 1

Introduction

The inconsistency of Newtonian mechanics with Maxwell's equation of electromagnetism led to the development of Special Relativity (SR). Theory of SR was introduced in 1905, by Albert Einstein, in his paper "On the Electrodynamics of Moving Bodies". He made major changes to mechanics to handle situations involving motions nearing speed of light. SR is based on two postulates. First, the laws of physics are invariant for all non-accelerating observer in all inertial frames. Second, the speed of light is constant in vacuum (not relative to the movement of the observer). The theory is special in a way that it only applies in the special case where the curvature of spacetime due to gravity is negligible. SR is restricted to the flat spacetime known as Minkowski spacetime [1]. Einstein introduced a theory of time, distance, mass and energy that was consistent with electromagnetism, but there was no force of gravity. In order to include gravity, Einstein introduced General Relativity (GR) in 1915.

GR is Einstein's theory of space, time and gravity. It was presented as a conceptual revolution in our views of space and time. He gave an idea that the three dimensions of space

and one dimension of time has bound together in single fabric of spacetime. The geometry of four dimensional spacetime can explain the motion of particles moving along surfaces of spacetime. This unified fabric is curved and stretched by heavy objects like planets and stars, and this curving of spacetime that creates what we feel as gravity. All bodies fall with the same acceleration in a gravitational field led Einstein to understand gravity in terms of curvature of spacetime. A planet like the Earth is kept in orbit because it follows a curve in a spacetime fabric caused by the Sun's presence.

GR generalizes special theory of relativity and Isaac Newton's theory of gravity or Newtonian mechanics. GR gives the understanding of astrophysical phenomena such as black hole, quasars, pulsars and Big Bang. It explains the motion of macroscopic objects and related phenomena such as bending of light due to gravity, gravitational redshift, peri-helion shift of Mercury, gravitational waves and gravitational time dilation.

Einstein gave a set of second order partial differential equations (discussed in Section 1.6)

$$R_{\mu\nu} - \frac{1}{2}Rg_{\mu\nu} - \Lambda g_{\mu\nu} = \kappa T_{\mu\nu}, \quad (\mu, \nu = 0, 1, 2, 3) \quad (1.1)$$

where

$$\kappa = \frac{8\pi G}{c^4},$$

known as the Einstein Field Equations (EFEs) with the cosmological constant Λ . These equations relate the curvature of the spacetime with the presence of mass, energy and momentum, collectively called stress-energy-momentum tensor $T_{\mu\nu}$. In (1.1) $R_{\mu\nu}$ is the Ricci tensor, R is its trace called the Ricci scalar and $g_{\mu\nu}$ is the metric tensor (all these tensors will be discussed in subsequent Sections).

Initially Einstein derived his equation without Λ . In 1917 Einstein added cosmological constant to his field equations to balance the gravitational pull of static universe. In 1920

Hubble made the discovery that the universe is expanding. He measured the distances and motion of galaxies. After this discovery, Einstein dropped cosmological constant from the EFEs. Later the cosmological constant came back in EFEs as a “dark energy”; a mysterious type of energy causing accelerated expansion of the universe [2].

The first exact solution to EFEs was found by Karl Schwarzschild in 1916. Schwarzschild solution [3] represents the spacetime geometry outside a static spherical symmetric matter distribution in the empty space. Vacuum solutions, electrovacuum solutions, null dust solutions, scalar field solution [4] are some of the exact solutions of EFEs. Reissner-Nordström (RN) metric [5, 6] was discovered soon after Schwarzschild metric. It was discovered by Mans Reissner and Gunnar Nordström. The RN is a static solution of the Einstein-Maxwell field equations which corresponds to the gravitational field of charged, spherically symmetric body of mass M . The exact solution for an uncharged, rotating black hole remained unsolved till 1963. Kerr metric describes the geometry of empty spacetime around a rotating uncharged axially symmetric black hole with ellipsoidal event horizon [7]. In 1965, Ezra Newmann found Kerr-Newmann (KN) metric [8]. The KN metric is a solution of the Einstein Maxwell field equations that describe the spacetime geometry in the region surrounding a charged, rotating mass [9].

The motion of a particle around black hole is one of the most important topics of black holes physics. The motion of a particle in the vicinity of black hole helps in understanding the geometry of spacetime near black hole. Due to the presence of gravitational field it is difficult for the particles to move on stable orbits which results in particle collisions, and different kinds of astrophysical phenomena [10, 11]. In this regard particle dynamics in different black hole spacetimes have been discussed by different authors. Israel studied the radial motion of the particle in the Schwarzschild spacetime and discussed the issue of gravitational collapse

[12]. In Schwarzschild spacetime, the relativistic motion of a test particle, released from rest at infinity appears to slow down as it fall towards the Schwarzschild black hole. It is known that the circular orbits in the Schwarzschild spacetime whose radii are less than three times the Schwarzschild radius are unstable, the stability of precessing elliptical orbits in the Schwarzschild field was discussed by Hansen in [13]. In [14] authors studied massive particles in a modified Schwarzschild geometry. Behaviour of spacelike geodesics in the extended Schwarzschild manifold was analyzed by Honig and Lake [15]. Ruffini and Denardo pointed out the existence of a generalized ergosphere in the Reissner-Nordström geometry and gives an explicit formula to determine its range. These results are compared with the case of the Kerr solutions [16]. Timelike and null geodesics in the RN spacetime were investigated by Dadhich and Kale in [17]. It was found that the incoming geodesics always encounter a turning point at a finite radial distance. The limits for escape, bound and stable orbits are obtained and shown to be closer to the source as compared with Schwarzschild spacetime [17]. Armenti studied the existence and stability criteria for circular geodesics in the vicinity of RN black hole [18]. Equatorial geodesic motions in the gravitational field of a rotating source was investigated by Felic [19]. He found orbital and vortical motion for Kerr black hole in [20]. Circular orbits in the Kerr metric were analyzed by Kurmakaer [21]. The behaviour of null geodesics, for extended Kerr manifolds was studied in [22]. Dadhich also calculated equatorial circular geodesics in the Kerr-Newmann (KN) spacetime [23]. The radial motion of the photons in the KN metric was given by Stuchlik in [24]. He found that the qualitative differences between the KN metric and Kerr metric occur only below the inner horizons and around naked singularities. In [25] Stuchlik and Hledik studied the equatorial photon motion in the KN spacetime with non-zero cosmological constant.

The first chapter consists of basic definitions, the derivation of EFEs by using the variational principle and an introduction to black holes. Throughout this thesis the signature of

the metric is $(-, +, +, +)$, $G = 1$ and $c = 1$.

Our main focus in this thesis is to investigate how particles behave in string cloud background during motion around Schwarzschild black hole. In chapter 2, an article entitled *Rindler modified Schwarzschild geodesic* [26] is reviewed, where the effect of the Rindler parameter on the motion of the particle is investigated and compared with the Schwarzschild geodesics.

In Chapter 3 we investigate the trajectories of the timelike and null geodesics for radial and circular motion of the Schwarzschild black hole in string cloud background. The effects of the string cloud parameter on the motion of the particle around Schwarzschild black hole is studied and is compared with the Schwarzschild geodesics. A conclusion is presented in chapter 4.

1.1 Metric Tensor

Metric tensor is defined as a bilinear map of two vectors into the real numbers (\mathfrak{R}) i.e we have set an equivalent expression for the inner product of two vectors V and W [27]

$$\begin{aligned} V \cdot W &= (V^\mu \vec{e}_\mu) \cdot (W^\nu \vec{e}_\nu), \\ &= V^\mu W^\nu (\vec{e}_\mu \cdot \vec{e}_\nu), \\ &= V^\mu W^\nu g_{\mu\nu}. \end{aligned}$$

Metric tensor is the dot product of basis vectors. It is symmetric by definition and its covariant and contravariant components are respectively

$$g_{\mu\nu} = g(e_\mu, e_\nu) = e_\mu \cdot e_\nu.$$

$$g^{\mu\nu} = g(e^\mu, e^\nu) = e^\mu \cdot e^\nu.$$

The metric tensor also defines the infinitesimal distance between two points on a curve $x^\mu(\lambda)$ and $x^\mu(\lambda + \Delta\lambda)$. If V^μ is the tangent vector field to the curve r then,

$$ds^2 = g(V, V)d\lambda^2 = g_{\mu\nu}V^\mu V^\nu d\lambda^2 = g_{\mu\nu}dx^\mu dx^\nu. \quad (1.2)$$

Here $V^\mu = \frac{dx^\mu}{d\lambda}$ and ds^2 is the line element of metric tensor $g_{\mu\nu}$. It is usually non degenerate, the determinant $g = |g_{\mu\nu}| \neq 0$. So, inverse of metric $g_{\mu\nu}$ exists and is unique, which yields

$$g_{\sigma\lambda}g^{\lambda\mu} = g^{\mu\nu}g_{\nu\sigma} = \delta^\mu{}_\sigma; \quad \mu, \nu, \sigma, \lambda = 0, 1, 2, 3. \quad (1.3)$$

Metric tensor $g_{\mu\nu}$ is a covariant symmetric tensor of rank two. A tensor is defined to be a scalar multi-linear function that maps vectors and one-forms into set of real numbers. A function is multi-linear if it is linear in all its arguments.

1.2 Geodesics

A geodesic is the curved space generalization of the notion of a straight line in Euclidean space. Geodesic is a curve along which the tangent vector is parallel transported. Let $x^\mu(\lambda)$ be the path and $\frac{dx^\mu}{d\lambda}$ is the tangent vector field to $x^\mu(\lambda)$. The condition that it be to parallel transported is thus [27]

$$\frac{d^2x^\mu}{d\lambda^2} + \Gamma^\mu{}_{\rho\sigma} \frac{dx^\rho}{d\lambda} \frac{dx^\sigma}{d\lambda} = 0. \quad (1.4)$$

Here Γ denotes Christoffel symbol, defined as

$$\Gamma^\mu{}_{\nu\lambda} = \frac{1}{2}g^{\mu\sigma} \left(g_{\sigma\lambda,\nu} + g_{\nu\sigma,\lambda} - g_{\nu\lambda,\sigma} \right). \quad (1.5)$$

We can consider the motion of freely falling particles. In flat space such particles move in straight lines, this is expressed as the vanishing of the second derivative of the parameterized

path $x^\mu(\lambda)$

$$a^\mu \equiv \frac{d^2 x^\mu}{d\lambda^2} = 0. \quad (1.6)$$

This is not a tensorial equation. Its tensorial form would be,

$$\frac{d^2 x^\mu}{d\lambda^2} = V^\nu \partial_\nu V^\mu = 0. \quad (1.7)$$

Now we can replace partial derivative by a covariant derivative to generalize this to curved space

$$V^\nu V^\mu{}_{;\nu} = 0. \quad (1.8)$$

Hence the general relativistic version of the Newtonian relation is simply the geodesic equations given by (1.4). Therefore, in GR free particles move along geodesics.

1.3 Riemann Tensor and Other Related Tensors

The Riemann tensor is also called curvature tensor because it describes the curvature of a spacetime in an invariant way. Riemann tensor is defined as [9]

$$R^\rho{}_{\sigma\mu\nu} = \Gamma^\rho{}_{\nu\sigma,\mu} - \Gamma^\rho{}_{\mu\sigma,\nu} + \Gamma^\rho{}_{\mu\lambda}\Gamma^\lambda{}_{\nu\sigma} - \Gamma^\rho{}_{\nu\lambda}\Gamma^\lambda{}_{\mu\sigma}, \quad (1.9)$$

the covariant form of Riemann tensor would be,

$$R_{\rho\sigma\mu\nu} = g_{\rho\lambda} R^\lambda{}_{\sigma\mu\nu}. \quad (1.10)$$

Let consider this tensor in locally inertial coordinates, at an arbitrary point 'p' in which the Christoffel symbol vanishes $\Gamma^a{}_{bc}|_p = 0$, but their derivatives will not. Therefore we may write

$$R_{\rho\sigma\mu\nu}(p) = \frac{1}{2} \left(g_{\rho\nu,\sigma\mu} - g_{\nu\sigma,\mu\rho} - g_{\rho\mu,\nu\sigma} + g_{\mu\sigma,\nu\rho} \right). \quad (1.11)$$

Riemann tensor is antisymmetric in its first and second pair of indices, i.e,

$$R_{\rho\sigma\mu\nu} = -R_{\sigma\rho\mu\nu}, \quad (1.12)$$

$$R_{\rho\sigma\mu\nu} = -R_{\rho\sigma\nu\mu}. \quad (1.13)$$

It is invariant under interchange of the second pair of indices with the first

$$R_{\rho\sigma\mu\nu} = R_{\mu\nu\rho\sigma}. \quad (1.14)$$

Following two Bianchi identities are satisfied by the Riemann tensor [9],

$$R^\rho{}_{\sigma\mu\nu} + R^\rho{}_{\mu\nu\sigma} + R^\rho{}_{\nu\sigma\mu} = 0. \quad (1.15)$$

$$R_{\rho\sigma\mu\nu;\lambda} + R_{\rho\sigma\nu\lambda;\mu} + R_{\rho\sigma\lambda\mu;\nu} = 0. \quad (1.16)$$

The Riemann tensor with four indices has n^4 independent components in an n dimensional space. Totally antisymmetric 4 index Riemann tensor has $\frac{1}{12}n^2(n^2 - 1)$ independent components [27, 28]. If the Riemann tensor vanishes; that is,

$$R^\rho{}_{\sigma\mu\nu} = 0, \quad (1.17)$$

than we can always construct a coordinate system in which the metric components are constant. Conversely, if a coordinate system exists in which the components of the metric are constant, the Riemann tensor will vanish.

Ricci tensor $R_{\sigma\nu}$ is the trace of the Riemann tensor

$$R_{\sigma\nu} \equiv R^\rho{}_{\sigma\rho\nu}, \quad (1.18)$$

is the only independent contraction; all others are either related to this, or vanishes. Ricci tensor is defined as;

$$R_{\sigma\nu} = \Gamma^\rho{}_{\sigma\nu,\rho} - \Gamma^\rho{}_{\sigma\rho,\nu} + \Gamma^\rho{}_{\lambda\rho}\Gamma^\lambda{}_{\sigma\nu} - \Gamma^\rho{}_{\lambda\nu}\Gamma^\lambda{}_{\sigma\rho}. \quad (1.19)$$

It is a symmetric tensor and its contraction gives the Ricci scalar, that is,

$$R = R^\nu{}_{\nu} = g^{\nu\sigma}R_{\sigma\nu}. \quad (1.20)$$

1.4 Einstein Tensor

Einstein tensor is a unique combination of Ricci tensor and Ricci scalar which describes the curvature of spacetime in EFEs of GR. It is divergence free and symmetric tensor. Einstein tensor could be derived from second Bianchi identity [9], raising the first index ρ and contracting it with ν . Using (1.12) for the second term

$$R_{\sigma\mu;\lambda} - R_{\sigma\lambda;\mu} + R^{\rho}{}_{\sigma\lambda\mu;\rho} = 0.$$

Raising σ , contracting it with λ ,

$$R^{\sigma}{}_{\mu;\sigma} - R_{;\mu} + R^{\rho\sigma}{}_{\sigma\mu;\rho} = 0.$$

Using symmetric property we have $R^{\rho\sigma}{}_{\sigma\mu;\rho} = R^{\rho}{}_{\mu;\rho}$ which implies

$$\begin{aligned} 2R^{\rho}{}_{\mu;\rho} - R_{;\mu} &= 0, \\ \left(2R^{\rho}{}_{\mu} - \delta^{\rho}{}_{\mu}R\right)_{;\rho} &= 0, \\ \left(R^{\rho\mu} - \frac{1}{2}g^{\rho\mu}R\right)_{;\rho} &= 0. \end{aligned}$$

The expression on the right hand side in the brackets is the Einstein tensor and is denoted by

$$\varepsilon^{\rho\mu} \equiv R^{\rho\mu} - \frac{1}{2}g^{\rho\mu}R. \quad (1.21)$$

1.5 Stress-Energy-Momentum Tensor

The stress-energy-momentum tensor describes the energy density and flux of energy and momentum in the spacetime. It is the source term in gravitational field equations. Stress-energy-momentum tensor is a second rank symmetric tensor, $T^{\mu\nu} = T^{\nu\mu}$. It describes the

matter and energy distribution at each point of the spacetime [27, 29]. Consider a local Cartesian inertial frame at P in which the set of components of the four-velocity of the fluid is $U^\mu = \gamma_\mu(c, \vec{u})$. The physical meaning of the components of $T^{\mu\nu}$ in this frame are [9].

- T^{00} is the energy density of the matter.
- T^{0i} is the energy flux in the i -direction.
- T^{i0} is the momentum density in the i -direction.
- T^{ij} is the rate of flow of the i -component of momentum per unit area in the j -direction.

For the derivation of stress-energy-momentum tensor, the Lagrangian for matter and energy is used. The stress-energy-momentum tensor is defined in section 1.7.

Example: In perfect fluid there are no forces between the particles, and has no heat conduction or viscosity in the instantaneous rest frame this implies $T^{0i} = T^{i0} = 0$ and $T^{ij} = 0$ if $i \neq j$, respectively. Thus, in IRF the components of $T^{\mu\nu}$ for the perfect fluid is defined as [9, 10]

$$T^{\mu\nu} = \left(\rho + \frac{P}{c^2}\right)U^\mu U^\nu - P g^{\mu\nu},$$

here ρ, P, U^μ are the energy density, pressure and four-velocity of the fluid respectively.

1.6 Derivation of Einstein Field Equations for Vacuum

EFEs are the set of second order partial differential equations for the metric tensor. EFEs describes the relation between the curvature of a spacetime and the energy and momentum of that spacetime. Action integral I_G , for the gravitational field and variation principal $\delta I_G = 0$,

would be used to drive EFEs. I_G is defined as [28, 30],

$$I_G = \frac{1}{2\kappa} \int_{\mathcal{V}} \mathcal{L}(g_{\mu\nu}, g_{\mu\nu,\lambda}) \sqrt{-g} d^4x. \quad (1.22)$$

Here $\kappa = 8\pi$ is a constant and calculated by the required condition that the EFEs reduce to Newton's law in the weak field limit. For the integral to be invariant under any transformation the function $\mathcal{L}(g_{\mu\nu})$ should be scalar. So, the gravitational field Lagrangian is

$$\mathcal{L}(g_{\mu\nu}, g_{\mu\nu,\lambda}) = R - 2\Lambda. \quad (1.23)$$

Use of (1.23) in (1.22) gives

$$\begin{aligned} I_G &= \frac{1}{2\kappa} \int_{\mathcal{V}} (R - 2\Lambda) \sqrt{-g} d^4x, \\ &= \frac{1}{2\kappa} \int_{\mathcal{V}} (g^{\mu\nu} R_{\mu\nu} - 2\Lambda) \sqrt{-g} d^4x, \\ &= \frac{1}{2\kappa} \int_{\mathcal{V}} (g^{\mu\nu} R_{\mu\nu} \sqrt{-g} - 2\Lambda \sqrt{-g}) d^4x. \end{aligned}$$

Now we will vary the action inside a infinitesimal region \mathcal{V} and assuming that the variation of the metric and its differentiation on the boundary of the region will vanish. Then we reduce the EFEs by the requirement that $\delta I_G = 0$, for any variation in the metric. From above equation we have,

$$\delta I_G = \frac{1}{2\kappa} \int_{\mathcal{V}} (g^{\mu\nu} \sqrt{-g} \delta R_{\mu\nu} + R_{\mu\nu} \delta [g^{\mu\nu} \sqrt{-g}] - 2\Lambda \delta \sqrt{-g}) d^4x. \quad (1.24)$$

Then in a local inertial frame the Ricci tensor will become

$$\begin{aligned} R_{\mu\nu} &= \Gamma^\lambda{}_{\mu\nu,\lambda} - \Gamma^\lambda{}_{\mu\lambda,\nu}, \\ \delta R_{\mu\nu} &= \delta \Gamma^\lambda{}_{\mu\nu,\lambda} - \delta \Gamma^\lambda{}_{\mu\lambda,\nu}. \end{aligned}$$

The partial derivative commute with the variation, i.e.

$$\delta R_{\mu\nu} = (\delta \Gamma^\lambda{}_{\mu\nu})_{;\lambda} - (\delta \Gamma^\lambda{}_{\mu\lambda})_{;\nu}.$$

Partial derivative of the metric tensor will vanish at boundary of \mathcal{V} . Then the last equation may be written as

$$g^{\mu\nu}\delta R_{\mu\nu} = (g^{\mu\nu}\delta\Gamma^\lambda{}_{\mu\nu} - g^{\mu\lambda}\delta\Gamma^\nu{}_{\mu\nu})_{;\lambda}$$

Introducing a vector A^λ ,

$$A^\lambda = g^{\mu\nu}\delta\Gamma^\lambda{}_{\mu\nu} - g^{\mu\lambda}\delta\Gamma^\nu{}_{\mu\nu},$$

then the above equation can be written as

$$g^{\mu\nu}\delta R_{\mu\nu} = A^\lambda{}_{;\lambda},$$

which is the total divergence. As the metric tensor and its derivative vanishes at the boundary then according to the Stokes theorem first term will vanish and contribute nothing to δI_G

$$\int_{\mathcal{V}} \left(g^{\mu\nu} \sqrt{-g} \delta R_{\mu\nu} \right) d^4x = 0. \quad (1.25)$$

Substituting (1.25) in (1.24), we obtain

$$\delta I_G = \frac{1}{2\kappa} \int_{\mathcal{V}} \left(R_{\mu\nu} \delta \left[g^{\mu\nu} \sqrt{-g} \right] - 2\Lambda \delta \sqrt{-g} \right) d^4x. \quad (1.26)$$

Further

$$\begin{aligned} \delta \sqrt{-g} &= \left[\frac{\partial \sqrt{-g}}{\partial g_{\alpha\beta}} \right] \delta g_{\alpha\beta} = -\frac{1}{2\sqrt{-g}} \left(\frac{\partial g}{\partial g_{\alpha\beta}} \right) \delta g_{\alpha\beta}, \\ \delta \sqrt{-g} &= \frac{1}{2} \sqrt{-g} g^{\alpha\beta} \delta g_{\alpha\beta}. \end{aligned} \quad (1.27)$$

Now

$$\delta \left[g^{\mu\nu} \sqrt{-g} \right] = \sqrt{-g} \delta g^{\mu\nu} + g^{\mu\nu} \delta \sqrt{-g},$$

we know $g^{\mu\beta} g_{\alpha\beta} = \delta^\mu_\alpha$ which gives

$$\delta(g^{\mu\alpha} g_{\alpha\beta}) = 0.$$

Hence we can write

$$\delta g_{\alpha\beta} = -g_{\alpha\mu} g_{\beta\nu} \delta g^{\mu\nu}.$$

This implies

$$\delta\left(g^{\mu\nu}\sqrt{-g}\right) = \sqrt{-g}\left(\delta g^{\mu\nu} + \frac{1}{2}g^{\mu\nu}g^{\alpha\beta}\delta g_{\alpha\beta}\right) = \sqrt{-g}\left(\delta g^{\mu\nu} - \frac{1}{2}g^{\mu\nu}g_{\alpha\beta}\delta g^{\alpha\beta}\right). \quad (1.28)$$

Substituting (1.27) and (1.28) in (1.26), gives the variation in the action that is

$$\delta S_G = \frac{1}{2\kappa} \int_{\mathcal{V}} \sqrt{-g} \left(R_{\alpha\beta} - \frac{1}{2} R g_{\alpha\beta} - \Lambda g_{\alpha\beta} \right) \delta g^{\alpha\beta} d^4x, \quad (1.29)$$

δS_G must be zero for the vacuum field equations of general theory of relativity. This implies

$$R_{\alpha\beta} - \frac{1}{2} R g_{\alpha\beta} - \Lambda g_{\alpha\beta} = 0; \quad \alpha, \beta = 0, 1, 2, 3. \quad (1.30)$$

Since $R_{\alpha\beta}$ and $g_{\alpha\beta}$ are symmetric, therefore (1.30) is a set of 10 partial differential equations.

1.7 The Einstein Field Equations in the Presence of Matter

We would derive the Einstein field equations in the presence of matter. Using the variational principle [9, 28]

$$\delta(S_G + S_M) = 0, \quad (1.31)$$

here S_M is the action integral for matter and energy. We derive the EFEs with energy-momentum tensor

$$S_M = \int_{\mathcal{V}} \mathcal{L}_M(g_{\mu\nu}, g_{\mu\nu,\lambda}) \sqrt{-g} d^4x, \quad (1.32)$$

here \mathcal{L}_M is the Lagrange density for matter

$$\delta[\sqrt{-g}\mathcal{L}_M] = \frac{\partial[\sqrt{-g}\mathcal{L}_M]}{\partial g^{\mu\nu}} \delta g^{\mu\nu} + \frac{\partial[\sqrt{-g}\mathcal{L}_M]}{\partial g^{\mu\nu},\lambda} \delta g^{\mu\nu},\lambda. \quad (1.33)$$

We define a vector B^λ as

$$B^\lambda \equiv \frac{\partial[\sqrt{-g}\mathcal{L}_M]}{\partial g^{\mu\nu},\lambda} \delta g^{\mu\nu}. \quad (1.34)$$

The divergence is $B^{\lambda, \lambda}$

$$B^{\lambda, \lambda} = \left[\frac{\partial[\sqrt{-g}\mathcal{L}_M]}{\partial g^{\mu\nu, \lambda}} \right]_{, \lambda} \delta g^{\mu\nu} + \frac{\partial[\sqrt{-g}\mathcal{L}_M]}{\partial g^{\mu\nu, \lambda}} \delta g^{\mu\nu, \lambda}. \quad (1.35)$$

Using (1.35) in (1.33), we get

$$\delta \left[\sqrt{-g}\mathcal{L}_M \right] = \frac{\partial[\sqrt{-g}\mathcal{L}_M]}{\partial g^{\mu\nu}} \delta g^{\mu\nu} - \left[\frac{\partial[\sqrt{-g}\mathcal{L}_M]}{\partial g^{\mu\nu, \lambda}} \right]_{, \lambda} \delta g^{\mu\nu} + B^{\lambda, \lambda}. \quad (1.36)$$

In our situation variation vanishes at the boundary so, by Gauss divergence theorem which implies $\int B^{\lambda, \lambda} d^4x = 0$, hence we have

$$\delta S_M = \int_{\mathcal{V}} \left(\frac{\partial[\sqrt{-g}\mathcal{L}_M]}{\partial g^{\mu\nu}} + \left[\frac{\partial[\sqrt{-g}\mathcal{L}_M]}{\partial g^{\mu\nu, \lambda}} \right]_{, \lambda} \right) \delta g^{\mu\nu} d^4x. \quad (1.37)$$

The energy-momentum tensor with Lagrange density is defined as

$$T_{\mu\nu} = -\frac{2}{\sqrt{-g}} \left(\frac{\partial[\sqrt{-g}\mathcal{L}_M]}{\partial g^{\mu\nu}} + \left[\frac{\partial[\sqrt{-g}\mathcal{L}_M]}{\partial g^{\mu\nu, \lambda}} \right]_{, \lambda} \right), \quad (1.38)$$

$$\delta S_M = -\frac{1}{2} \int_{\mathcal{V}} T_{\mu\nu} \sqrt{-g} \delta g^{\mu\nu} d^4x. \quad (1.39)$$

From (1.29) and (1.39) we get

$$R_{\mu\nu} - \frac{1}{2} g_{\mu\nu} R - \Lambda g_{\mu\nu} = \kappa T_{\mu\nu}. \quad (1.40)$$

These are the EFEs with stress-energy-momentum tensors. The L.H.S of the (1.40) gives the information about the curvature of the spacetime and the R.H.S describes the behaviour and location of matter.

1.8 Black Holes

Black hole is one of the most interesting objects in the sky. It arises from a stellar collapse or appear as the remnant of a supernova. Supernova explosion occurs when even larger

and hotter stars reach the end of their life. These stars are hot enough to burn Hydrogen, Helium, Carbon, Oxygen and Silicon as fuel. Eventually, the fusion in these stars forms the element iron, which effectively ends the nuclear fusion process within the star. Lacking fuel for fusion, the temperature decreases and the rate of collapse due to gravity increases, until it collapses completely [10]. If the mass of the compressed remnant of the star exceeds about three, four solar masses, then even the degeneracy pressure of neutrons is insufficient to halt the collapse and the core collapses completely into a gravitational singularity. The gravity of a single point containing all the mass of the entire original star becomes so strong that even light can not escape from it. The region of spacetime having strong gravitational effects that nothing can escape from inside it, neither particles nor light, is known as a black hole.

After the creation of the black hole, the heat and the hugely amplified magnetic field of the collapsing star combine to focus a pair of tight beams or jets of radiation, perpendicular to the spinning plane of the accretion disk. The shock waves of this massive energetic beam cause gamma rays to be emitted in a phenomenon known as a gamma ray burst [10].

Black holes are invisible because the light can not escape through them, so the different behaviour of the stars that are very close to the black holes indicates their presence.

Mathematically black holes are the singular solutions of the EFEs. The first exact black hole solution of EFEs is the Schwarzschild solution. The line element is [9]

$$ds^2 = -\left(1 - \frac{2M}{r}\right)dt^2 + \frac{1}{\left(1 - \frac{2M}{r}\right)}dr^2 + r^2(d\theta^2 + \sin^2\theta d\phi^2). \quad (1.41)$$

The metric coefficients g_{tt} and g_{rr} become infinite at $r = 0$ and $r = 2M$ (M is the mass of the black hole), respectively. The metric coefficients are coordinate dependent quantities

and one should not take too much of their values, it is certainly possible to have a coordinate singularity that results from a breakdown of a specific coordinate system rather than underlying manifold [27].

The curvature is measured by Riemann tensor and it is difficult to know where tensor becomes infinite, since its components are coordinate dependent. But we can construct various scalar quantities from curvature i.e, $R = g^{\mu\nu} R_{\mu\nu}$ or higher order scalars such as $R^{\mu\nu\rho\sigma} R_{\mu\nu\rho\sigma}$, $R_{\mu\nu\rho\sigma} R^{\rho\sigma\lambda\tau} R_{\lambda\tau} R^{\mu\nu}$, and so on. Since scalars are coordinate independent so it is easy to say that they become infinite. If any of these scalars goes to infinity as we approach some point, that point is regarded as a singularity of the curvature. In the case of the Schwarzschild solution direct calculations reveals that

$$R^{\mu\nu\rho\sigma} R_{\mu\nu\rho\sigma} = \frac{48M^2}{r^6}.$$

This shows that $r = 0$, is a curvature singularity representing the discontinuity in the fabric of spacetime [27]. The coordinate singularity is at $r = 2M$, the Schwarzschild radius. One could check that none of the curvature invariants blows up there. Therefore, one could think that it is actually not singular, but simply bad coordinate system is chosen. To remove this singularity one should transform to more appropriate coordinates if possible (see for detail e.g [27]).

1.9 Singularity

Singularities are those regions of spacetime where the paths of light and falling particles comes to an abrupt end, quantities that are used to measure gravitational field become infinite and geometry becomes undefined [9, 10]. Curvature singularity and coordinate singularity are

two types of singularities. Singularities can also be divided according to whether they are covered by event horizon or not (naked singularity).

Coordinate singularity occurs when an apparent singularity or discontinuity occurs in one coordinate system, and can be removed by choosing a different coordinate system. But the curvature singularity cannot be removed because it represents discontinuity in spacetime fabric. As explained in the previous section if Ricci scalar goes to infinity as we approach some point than that point is known as curvature singularity. For example in Schwarzschild black hole $r = 0$ is the curvature singularity and $r = 2M$ is the coordinate singularity (discussed in section 1.8).

1.10 Event Horizon

The black hole is surrounded by a well defined surface or edge known as event horizon. Inside the event horizon nothing can be seen and nothing can escape. The event horizon of a black hole is the point of no return. In other words, space itself is falling into the black hole at a speed greater than the speed of light [9]. For example if we consider the Schwarzschild black hole than, mathematically, the event horizon of the Schwarzschild black hole could be obtained by putting the coefficient of time coordinate of Schwarzschild metric (1.41) equal to zero, that is;

$$g_{tt} = 1 - \frac{2M}{r_h} = 0,$$

or

$$r_h = 2M.$$

Chapter 2

Rindler Modified Schwarzschild Geodesics

This chapter is devoted to a review of the “Rindler modified Schwarzschild geodesics” [26]. The effect of the Rindler parameter on the trajectories of timelike and null geodesics is investigated and compared with the Schwarzschild geodesics.

Rindler acceleration affects all massive and massless particles. As Rindler force is constant so one can also take it as a perturbation due to other forces. The non-isotropic role of Rindler parameter a makes it different from cosmological constant as we follow from the paper [26]. Since, Rindler acceleration refers to large distances so it is not necessary for the central object to be a black hole.

In [26] trajectories of the timelike and null geodesics in the presence of Rindler acceleration were investigated. It was noticed that if Rindler acceleration vanishes the result reduces to

Schwarzschild case. The physical effects of the model proposed by Grumiller were investigated in [31]. In that study, prehelion shift, light bending and gravitational redshift were calculated for solar system planets in the presence of Rindler parameter. Although, it remains to investigate the physical source that gives raise to such a term.

This chapter is organised as follows. In Section 2.1, the derivation of the particle trajectories and effective potential in Grumiller spacetime is done. In Section 2.2, the derivations of the trajectories of the timelike and null geodesics for radial motion in Grumiller spacetime is done, and the plots are also presented. In Section 2.3, the derivations of the trajectories of the timelike and null geodesics for circular motion in Grumiller spacetime along with their plots are presented.

Structure of Grumiller spacetime

Grumiller has proposed a model for gravity at large distances of a central object by assuming static and spherically symmetric system. The corresponding line element in the absence of cosmological constant is [26]

$$ds^2 = -f(r)dt^2 + \frac{1}{f(r)}dr^2 + r^2(d\theta^2 + \sin^2\theta d\phi^2), \quad (2.1)$$

where

$$f(r) = 1 - \frac{2M}{r} + 2ar. \quad (2.2)$$

Here M is the mass of the central object and a is the Rindler acceleration parameter which is a real number. The horizons of (2.1) are obtained by

$$f(r) = 1 - \frac{2M}{r_h} + 2ar_h = 0,$$

which yields

$$r_{h\pm} = \frac{-1 \pm \sqrt{1 + 16Ma}}{4a}, \quad (2.3)$$

considering the positive value of r_h

$$r_h = \frac{-1 + 1 + 8Ma - 32M^2a^2 + \dots}{4a},$$

neglecting higher order terms we have

$$r_h = 2M - 8M^2a.$$

In the presence of Rindler acceleration the radius of the horizon is smaller than the Schwarzschild horizon without Rindler parameter. Now if $a \rightarrow 0$, we get $r_h = 2M$, which is the Schwarzschild black hole horizon.

2.1 Particle Trajectories

For the spacetime given by (2.1) the geodesic Lagrangian for particle is given by

$$\mathcal{L} = \frac{m}{2} g_{\mu\nu} \dot{x}^\mu \dot{x}^\nu = m \left(-\frac{1}{2} f(r) \dot{t}^2 + \frac{\dot{r}^2}{2f(r)} + \frac{1}{2} r^2 (\dot{\theta}^2 + \sin^2 \theta \dot{\phi}^2) \right). \quad (2.4)$$

Throughout this dissertation dot denotes derivative with respect to the geodetic parameter τ .

The Euler-Lagrange equations are

$$\frac{d}{d\lambda} \left(\frac{\partial \mathcal{L}}{\partial \dot{x}^\mu} \right) - \frac{\partial \mathcal{L}}{\partial x^\mu} = 0, \quad (\mu = 0, 1, 2, 3) \quad (2.5)$$

For $\mu = 0$, (2.5) gives,

$$\begin{aligned} \frac{\partial \mathcal{L}}{\partial t} = 0 &\Rightarrow \frac{d}{d\lambda} \left(\frac{\partial \mathcal{L}}{\partial \dot{t}} \right) = 0, \\ \frac{d}{d\lambda} \left(\frac{\partial \mathcal{L}}{\partial \dot{t}} \right) &= \frac{d}{d\lambda} \left(-f(r) \dot{t} \right). \end{aligned}$$

Integrating with respect to λ , we obtain

$$-f(r) \dot{t} = \text{constant} = \frac{\varepsilon}{m} = E,$$

where E is constant of integration. We are considering static spherically symmetric spacetime and invariance under time translation leads to conservation of energy, so here the conserved quantity is the the energy per unit mass of the particle. The last equation can be arranged as

$$\dot{t} = \frac{-\varepsilon}{f(r)m} = \frac{-E}{f(r)}. \quad (2.6)$$

For $\mu = 3$, (2.5) becomes

$$\frac{d}{d\lambda} \left(\frac{\partial \mathcal{L}}{\partial \dot{\phi}} \right) - \frac{\partial \mathcal{L}}{\partial \phi} = 0,$$

since

$$\frac{\partial \mathcal{L}}{\partial \phi} = 0 \Rightarrow \frac{d}{d\lambda} \left(\frac{\partial \mathcal{L}}{\partial \dot{\phi}} \right) = 0,$$

$$\frac{d}{d\lambda} \left(2\dot{\phi} r^2 \sin^2 \theta \right) = 0,$$

$$2\dot{\phi} r^2 \sin^2 \theta = \text{constant},$$

$$\dot{\phi} r^2 \sin^2 \theta = \text{constant} = \frac{l}{m} = L, \quad (2.7)$$

where L is constant of integration. We have static spherical symmetric spacetime and invariance under spatial rotation leads to the conservation of the angular momentum, so here the conserved quantity is the magnitude of the angular momentum. Conservation of the direction of the angular momentum means that the particle is moving in a plane. We can choose this to be the equatorial plane of our coordinate system. In the equatorial plane, $\theta = \frac{\pi}{2}$, we get $L = r^2 \dot{\phi}$.

We know the normalization condition for four-velocity as

$$g_{\mu\nu} \frac{dx^\mu}{d\lambda} \frac{dx^\nu}{d\lambda} = -\epsilon. \quad (2.8)$$

In the equatorial plane, $\theta = \frac{\pi}{2}$, (2.8) implies

$$-f(r)\dot{t}^2 + \frac{\dot{r}^2}{f(r)} + r^2\dot{\phi}^2 = -\epsilon,$$

Using (2.6) and (2.7) we get

$$\left(\frac{dr}{d\lambda}\right)^2 = E^2 - f(r)\left(\epsilon + \frac{L^2}{r^2}\right), \quad (2.9)$$

$$\frac{1}{2}\left(\frac{dr}{d\lambda}\right)^2 + V_{eff}(r) = \frac{1}{2}E^2, \quad (2.10)$$

here $V_{eff}(r) = \frac{1}{2}f(r)\left(\epsilon + \frac{L^2}{r^2}\right)$, is the effective potential and the corresponding effective energy is

$$E_{eff} = \frac{1}{2}E^2.$$

The effective potential can be written as

$$V_{eff}(r) = \frac{1}{2}\left(1 - \frac{2M}{r} + 2ar\right)\left(\epsilon + \frac{L^2}{r^2}\right). \quad (2.11)$$

$$V_{eff}(r) = \frac{\epsilon}{2} - \frac{M\epsilon}{r} + \frac{L^2}{r^2} - \frac{ML^2}{r^3} + ar\left(\epsilon + \frac{L^2}{r^2}\right).$$

The first term in effective potential is constant, the second term corresponds to the Newtonian gravitational potential, the third term the centrifugal barrier, the fourth term the GR correction, and the last term proportional to the Rindler acceleration a . If $a \rightarrow 0$, the behaviour of geodesics remain identical to Schwarzschild case. But as a increases its affect is added to the potential.

2.2 Radial Motion

For radial motion $\phi = \text{constant}$, this implies $L = 0$. By substituting $L = 0$ in (2.9) we have

$$\left(\frac{dr}{d\lambda}\right)^2 = E^2 - \epsilon f(r). \quad (2.12)$$

Equation (2.12) is the general equation for radial motion. Now we will find null and timelike geodesics for radial motion.

2.2.1 Null Geodesics

The trajectory of a photon is a null geodesic. For massless particles, which move along null trajectories, we always have $\epsilon = 0$ in (2.8). Taking an arbitrary affine parameter, the equation (2.12) for null geodesics becomes

$$\left(\frac{dr}{d\lambda}\right)^2 = E^2. \quad (2.13)$$

Using (2.6) in (2.13) we arrive at

$$\begin{aligned} \left(\frac{dr}{d\lambda}\right)^2 &= \left(-f(r)\frac{dt}{d\lambda}\right)^2, \\ \frac{dr}{dt} = f(r) &= \pm\left(1 - \frac{2M}{r} + 2ar\right), \end{aligned}$$

By integrating, we get

$$\pm(t - t_0) = \frac{\ln\left(\frac{r-2M+2ar^2}{r_0-2M+2ar_0^2}\right)}{4a} + \frac{\left[\tanh^{-1}\left(\frac{1+4ar}{\sqrt{16Ma+1}}\right) - \tanh^{-1}\left(\frac{1+4ar_0}{\sqrt{16Ma+1}}\right)\right]}{2a\sqrt{16Ma+1}}. \quad (2.14)$$

Here t_0 and r_0 is the initial time and initial position of the massless particle respectively while t is the time measured by a distant observer. If we take $a = 0$, the photon worldlines will have slopes ± 1 as if $r \rightarrow \infty$, and their slopes approach to $\pm\infty$ as r approach to the Schwarzschild black hole horizon.

2.2.2 Timelike Geodesics

In the case of timelike geodesics (i.e $\epsilon = 1$) which refers to the motion of a massive particles. We can choose affine parameter to be the proper time τ . For timelike geodesics (2.12) becomes

$$\left(\frac{dr}{d\tau}\right)^2 = E^2 - 1 + \frac{2M}{r} - 2ar. \quad (2.15)$$

Now first we find the radial equation of motion by using Euler-Lagrange equation

$$\frac{d}{d\tau} \left(\frac{\partial \mathcal{L}}{\partial \dot{r}} \right) - \frac{\partial \mathcal{L}}{\partial r} = 0, \quad (2.16)$$

Consider (2.4) in equatorial plane.

$$\frac{\partial \mathcal{L}}{\partial r} = \left(\frac{-M}{r^2} - a \right) \dot{t}^2 - \frac{1}{f(r)^2} \left(\frac{M}{r^2} + a \right) \dot{r}^2. \quad (2.17)$$

$$\frac{\partial \mathcal{L}}{\partial \dot{r}} = \frac{\dot{r}}{f(r)},$$

$$\frac{d}{d\tau} \left(\frac{\partial \mathcal{L}}{\partial \dot{r}} \right) = \frac{f(r)\ddot{r} - \dot{r}^2 \left(\frac{2M}{r^2} + 2a \right)}{[f(r)]^2}. \quad (2.18)$$

Now using (2.17) and (2.18) in (2.16), we get

$$\frac{\ddot{r}}{f(r)} - \frac{\dot{r}^2 \left(\frac{M}{r^2} + a \right)}{[f(r)]^2} + \left(\frac{M}{r^2} + a \right) \dot{t}^2 - r \dot{\phi}^2 = 0. \quad (2.19)$$

In this case of radial motion $\dot{\phi} = 0$, thus (2.19) becomes

$$\frac{\ddot{r}}{f(r)} - \frac{\dot{r}^2 \left(\frac{M}{r^2} + a \right)}{[f(r)]^2} + \left(\frac{M}{r^2} + a \right) \dot{t}^2 = 0. \quad (2.20)$$

Inserting (2.15) and (2.6) in (2.20) we have

$$\frac{\ddot{r}}{f(r)} - \frac{(E^2 - f(r)) \left(\frac{M}{r^2} + a \right)}{[f(r)]^2} + \left(\frac{M}{r^2} + a \right) \left(\frac{-E}{f(r)} \right)^2 = 0,$$

we obtain

$$\frac{d^2 r}{d\tau^2} = -\frac{M}{r^2} - a. \quad (2.21)$$

Now let us consider the particle initially at rest and, upon the gravitational attraction, starts moving from its radial location $r = r_0$, using

$$\left(\frac{dr_0}{d\tau} \right)^2 = E^2 - 1 + \frac{2M}{r_0} - 2ar_0,$$

as r_0 is the initial radial position,

$$0 = E^2 - 1 + \frac{2M}{r_0} - 2ar_0,$$

$$E^2 = 1 - \frac{2M}{r_0} + 2ar_0, \quad (2.22)$$

Substituting (2.22) in (2.15)

$$\begin{aligned} \left(\frac{dr}{d\tau}\right)^2 &= \left(1 - \frac{2M}{r_0} + 2ar_0\right) - \left(1 - \frac{2M}{r} + 2ar\right), \\ \left(\frac{dr}{d\tau}\right)^2 &= \left(1 - \frac{2M}{r_0} + 2ar_0 - 1 + \frac{2M}{r} - 2ar\right), \\ \left(\frac{dr}{d\tau}\right)^2 &= 2M\left(\frac{1}{r} - \frac{1}{r_0}\right) + 2a(r_0 - r). \end{aligned} \quad (2.23)$$

From (2.11) the effective potential in radial motion for massive particles reads

$$V_{eff}(r) = \frac{1}{2}\left(1 - \frac{2M}{r} + 2ar\right). \quad (2.24)$$

In figure 2.1 $V_{eff}(\tilde{r}) = \frac{1}{2}(1 - \frac{2}{\tilde{r}} + 2\tilde{a}\tilde{r})$ is plotted by introducing $\frac{r}{M} = \tilde{r}$, $Ma = \tilde{a}$ against \tilde{r} . Here the intersection of $V_{eff}(\tilde{r})$ with \tilde{r} shows the horizon \tilde{r}_h . There is an upper bound for the motion of the particle in the presence of the Rindler parameter. The effective potential increases with the increasing value of Rindler acceleration parameter.

Substituting (2.6) in (2.15)

$$\begin{aligned} \left(\frac{dr}{d\tau}\right)^2 &= f(r)^2 \left(\frac{dt}{d\tau}\right)^2 - 1 + \frac{2M}{r} - 2ar, \\ \frac{\left(\frac{dr}{d\tau}\right)^2}{\left(\frac{dt}{d\tau}\right)^2} &= \frac{f(r)^2 \left(\frac{dt}{d\tau}\right)^2}{\left(\frac{dt}{d\tau}\right)^2} + \frac{-1 + \frac{2M}{r} - 2ar}{\left(\frac{dt}{d\sigma}\right)^2}, \\ \left(\frac{dr}{dt}\right)^2 &= f(r)^2 + \left(-1 + \frac{2M}{r} - 2ar\right) \left(\frac{d\tau}{dt}\right)^2, \\ \left(\frac{dr}{dt}\right)^2 &= \frac{1}{E^2} \left(E^2 - 1 + \frac{2M}{r} - 2ar\right) \left(1 - \frac{2M}{r} + 2ar\right)^2. \end{aligned} \quad (2.25)$$

Differentiating (2.25) with respect to t , and simplifying, we get the acceleration of the particle with respect to coordinate time t

$$\frac{d^2r}{dt^2} = -\frac{12}{E^2 r^4} \left(M + ar^2\right) \left(M - ar^2 - \frac{r}{2}\right) \left(M + \left(\frac{E^2}{3} - \frac{1}{2}\right)r - ar^2\right).$$

Here t is the time measured by the distant observer.

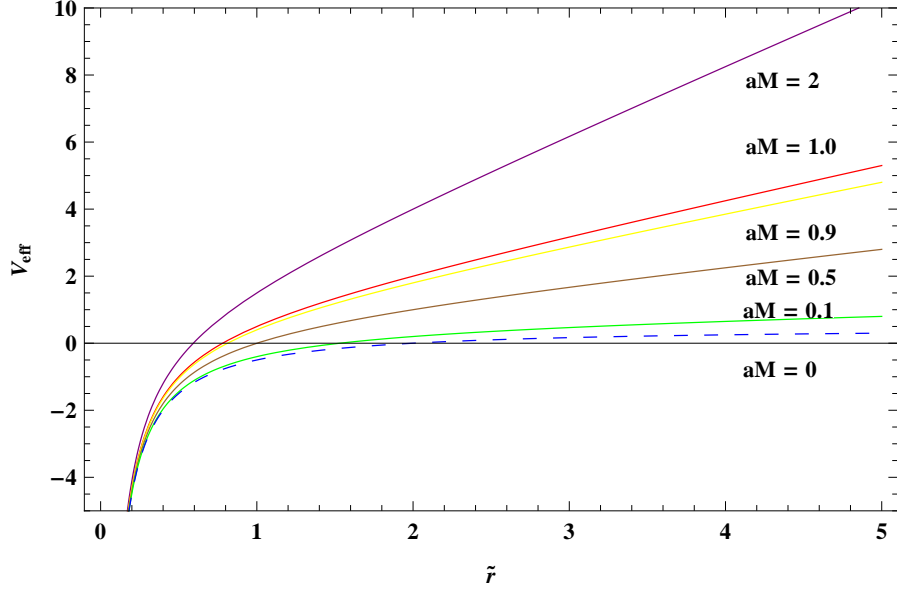


Figure 2.1: The effective potential $V_{eff}(\tilde{r})$ rises with the increasing \tilde{a} . This behaviour serves to confine geodesics nearer to the gravitating center.

2.3 Circular Motion

In this section circular motion of a photon and massive particles is studied. For circular motion in the equatorial plane we have $r = \text{constant}$, and hence $\dot{r} = \ddot{r} = 0$. For convenience, $r = \frac{1}{u}$ is introduced. By considering $\frac{du}{d\phi}$ at $u = u_c$ is zero in which $r_c = \frac{1}{u_c}$ is the circular orbit of the particle.

Using chain rule,

$$\dot{r} = \frac{dr}{d\sigma} = \frac{dr}{d\phi} \frac{d\phi}{d\sigma} = \frac{dr}{d\phi} \frac{L}{r^2},$$

(2.9) becomes,

$$\begin{aligned} \left(\frac{du}{d\phi}\right)^2 &= \frac{E^2}{L^2} - \left(1 - 2Mu + \frac{2a}{u}\right) \left(\frac{\epsilon}{L^2} + u^2\right), \\ \left(\frac{du}{d\phi}\right)^2 &= \frac{E^2}{L^2} - \frac{\epsilon}{L^2} - u^2 + \frac{2M\epsilon u}{L^2} + 2Mu^3 - \frac{2a\epsilon}{uL^2} - 2au, \end{aligned} \quad (2.26)$$

taking derivative of both sides with respect to ϕ ,

$$\frac{d^2u}{d\phi^2} = -u + \frac{M\epsilon}{L^2} + 3Mu^2 + \frac{a\epsilon}{u^2L^2} - a.$$

At $u = u_c$,

$$\frac{E^2}{L^2} - \left(1 - 2Mu_c + \frac{2a}{u_c}\right) \left(\frac{\epsilon}{L^2} + u_c^2\right) = 0. \quad (2.27)$$

In the circular motion we have $\frac{d^2u}{d\phi^2} = 0$, therefore, from (2.27) we have,

$$\frac{d}{du} \left[\frac{E^2}{L^2} - \left(1 - 2Mu + \frac{2a}{u}\right) \left(\frac{\epsilon}{L^2} + u^2\right) \right]_{u=u_c} = 0. \quad (2.28)$$

These conditions give the expression for the angular momentum.

$$-u_c + \frac{M\epsilon}{L^2} + 3Mu_c^2 + \frac{a\epsilon}{u_c^2L^2} - a = 0,$$

solving for L^2 gives,

$$L^2 = \frac{\epsilon(Mu_c^2 + a)}{u_c^2(u_c - 3Mu_c^2 + a)}. \quad (2.29)$$

Energy of the particle: Substitution of the above expression in (2.27) implies

$$\begin{aligned} 0 = & \frac{E^2}{L^2} - \epsilon \left(\frac{u_c^2(u_c - 3Mu_c^2 + a)}{\epsilon(Mu_c^2 + a)} \right) - u_c^2 + 2M\epsilon u_c \left(\frac{u_c^2(u_c - 3Mu_c^2 + a)}{\epsilon(Mu_c^2 + a)} \right) + 2Mu_c^3 \\ & - 2a\epsilon \left(\frac{u_c(u_c - 3Mu_c^2 + a)}{\epsilon(Mu_c^2 + a)} \right) - 2au_c, \end{aligned}$$

solving for E^2 , we get

$$E^2 = \frac{4\epsilon(a + \frac{u_c}{2} - Mu_c^2)^2}{u_c(a + u_c - 3Mu_c^2)}. \quad (2.30)$$

Here the value of circular geodesic is bounded. For physically acceptable motion the constraint $a + u_c - 3Mu_c^2 > 0$ arises from (2.29) this implies

$$r_c^2 a + r_c - 3M > 0,$$

which yields

$$r_c > \frac{-1 + \sqrt{1 + 12Ma}}{2a} = r_{cmin}.$$

here r_{cmin} is larger than the horizon

$$r_h = \frac{-1 + \sqrt{1 + 16Ma}}{4a}.$$

Hence,

$$\begin{aligned} r_{cmin} - r_h &= \frac{-1 + \sqrt{1 + 12Ma}}{2a} - \frac{-1 + \sqrt{1 + 16Ma}}{4a}, \\ &= \frac{2\sqrt{1 + 12Ma} - \sqrt{1 + 16Ma} - 1}{4a} > 0, \end{aligned}$$

The geodesic equation $r^2\dot{\phi} = L$ can not be satisfied for circular orbits with $r < \frac{-1 + \sqrt{1 + 12Ma}}{2a}$. Since they do not satisfy geodesic equations hence these orbits are not geodesics and cannot followed by freely falling particles. It is concluded that circular orbit cannot be maintained by a free massive particle with $r < \frac{-1 + \sqrt{1 + 12Ma}}{2a}$ around spherical massive body. In figure 2.2 we plot $\frac{r_{cmin} - r_h}{M}$ versus Ma , which implies that with larger value of Rindler parameter, r_{cmin} approaches to r_h . The gap between r_{cmin} and r_h gets smaller, but it always remains positive.

2.3.1 Null Geodesics

From (2.29) it is clear that only possible radius for circular photon orbit is

$$\frac{1}{r_c} - \frac{3M}{r_c^2} + a = 0,$$

which gives,

$$r_c = \frac{-1 \pm \sqrt{1 + 12Ma}}{2a}. \tag{2.31}$$

In this case from (2.27)

$$\frac{E^2}{L^2} = \left(1 - 2Mu_c + \frac{2a}{u_c}\right) \left(u_c^2\right),$$

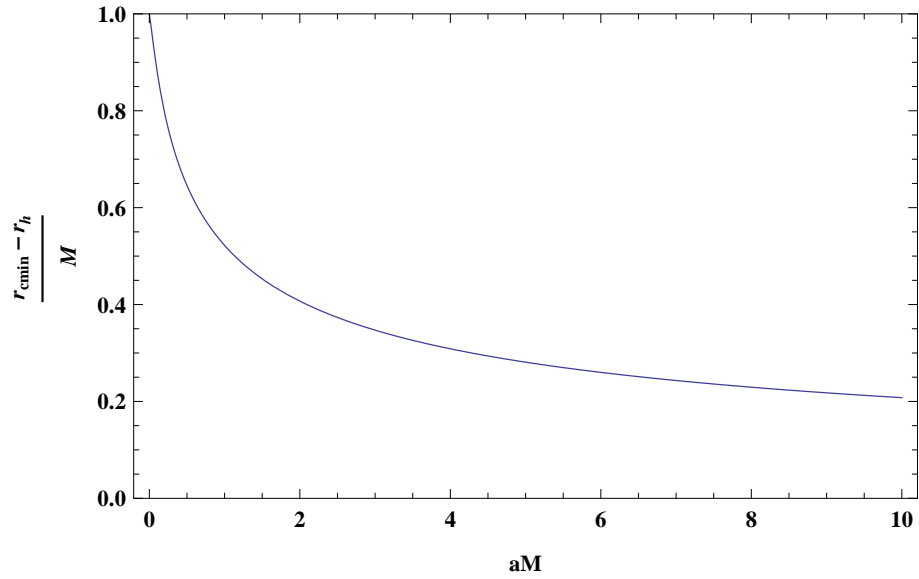


Figure 2.2: The difference between circular geodesics radii and horizon radii is shown as a function of aM . For increasing aM , the circular geodesics approach to the horizon.

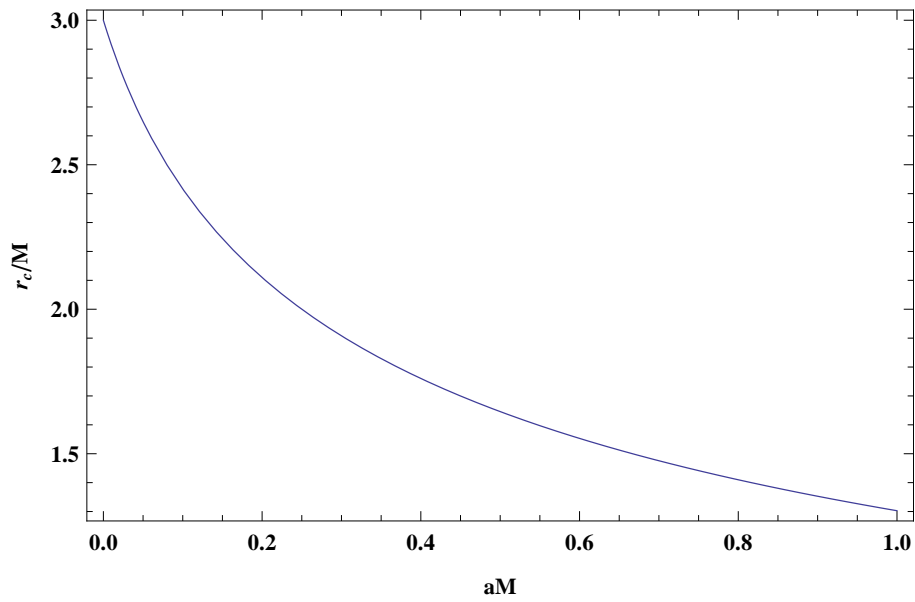


Figure 2.3: Plot of $\frac{r_c}{M}$ versus aM for a massless particle.

$$\frac{E^2}{L^2} = \frac{1}{r_c^2} - \frac{2M}{r_c^3} + \frac{2a}{r_c}.$$

Substituting the value of $r_c = \frac{-1 \pm \sqrt{1+12Ma}}{2a}$ in above equation gives,

$$\frac{E^2}{L^2} = \frac{(1 + \sqrt{1 + 12Ma} + 24Ma)(1 + \sqrt{1 + 12Ma})}{108M^2}. \quad (2.32)$$

In figure 2.3 we plot $\frac{r_c}{M}$ versus aM (for unit mass M). This shows that for larger value of Rindler parameter a the circular orbit of photon has smaller radius. In figure 2.4, $\frac{E^2}{L^2 M^2}$ is plotted against aM (for unit mass M). It is clear that for larger value of a the circular orbit of photon has larger value of $\frac{E^2}{L^2}$.

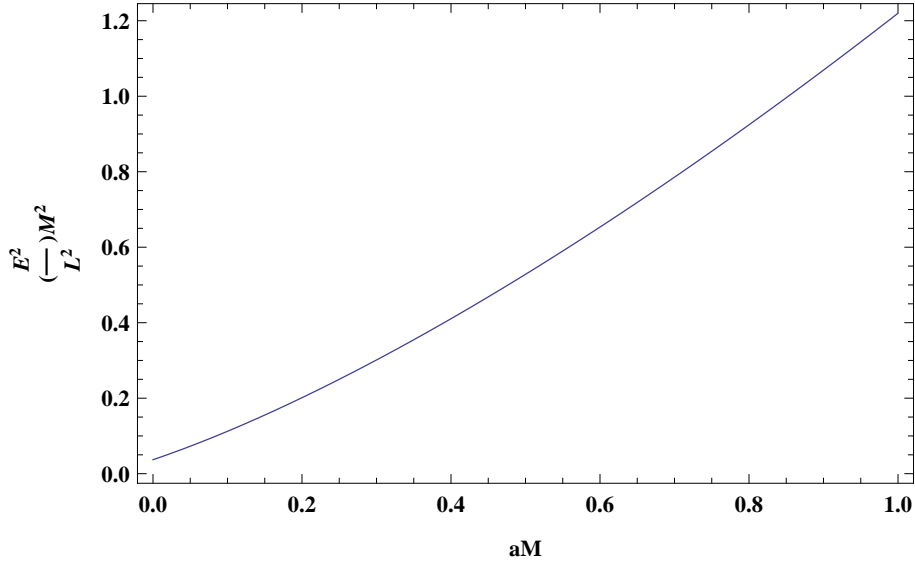


Figure 2.4: Plot of $\left(\frac{E^2}{L^2}\right)M^2$ versus aM for a massless particle ($M = 1$).

Stability: Replace $\tau = \frac{\tilde{\tau}}{L}$ in (2.10) gives

$$\left(\frac{dr}{d\tilde{\tau}}\right)^2 + V_{eff}(r) = E_{eff}(r),$$

here

$$V_{eff}(r) = \frac{f(r)}{r^2} = \frac{1 - \frac{2M}{r} + 2ar}{r^2},$$

$$V_{eff}(r) = \frac{r - 2M + 2ar^2}{r^3},$$

and

$$E_{eff}(r) = \frac{E^2}{L^2}.$$

For stable circular orbit we must have $V'_{eff} = 0$ and $V''_{eff} > 0$ at r_c

$$V''_{eff} = \frac{6}{r_c^4} - \frac{24M}{r_c^5} + \frac{4a}{r_c^3},$$

$$V''_{eff} = 6 \left(\frac{2a}{-1 + \sqrt{1 + 12Ma}} \right)^4 - 24M \left(\frac{2a}{-1 + \sqrt{1 + 12Ma}} \right)^5 + 4a \left(\frac{2a}{-1 + \sqrt{1 + 12Ma}} \right)^3. \quad (2.33)$$

Considering unit mass M , and for $a = 0.1$, (2.33) becomes

$$V''_{eff} = -0.08724,$$

for $a = 0.5$, (2.33) becomes

$$V''_{eff} = -0.715848,$$

for $a = 0.9$, (2.33) becomes

$$V''_{eff} = -2.0473.$$

Hence, V''_{eff} gives negative value so there is no stable circular orbit for photons. The local maxima in the potential curves are the locations of unstable circular orbits. As shown in figure 2.5 there is no stable circular orbit for photons for different values of Rindler acceleration parameter.

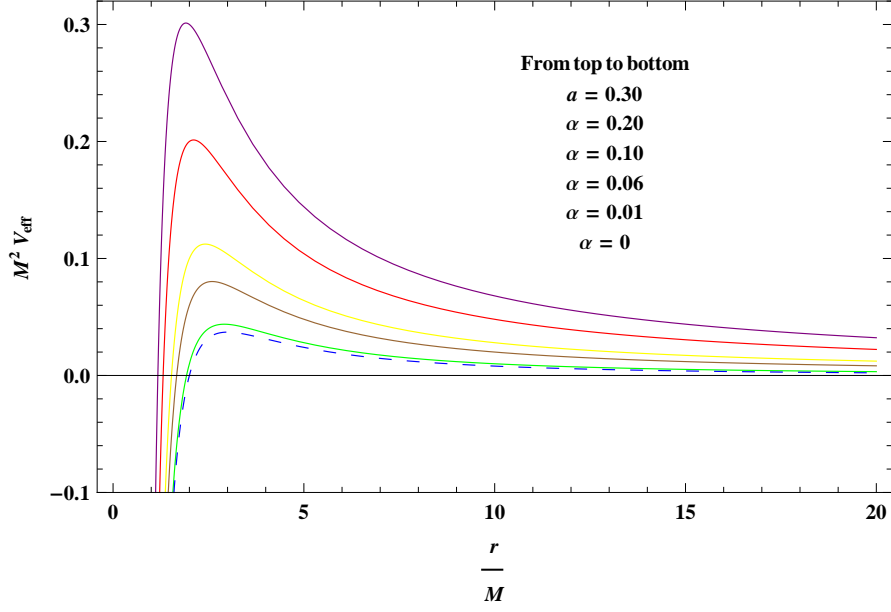


Figure 2.5: Plot of $M^2 V_{eff}$ versus $\frac{r}{M}$ for photon shows the unstable circular orbits for photons. In this range of aM no stable photon orbit exist.

2.3.2 Timelike Geodesics

Similarly for timelike geodesics (2.29) gives the angular momentum of the massive particle.

$$L^2 = \frac{(Mu_c^2 + a)}{u_c^2(u_c - 3Mu_c^2 + a)}. \quad (2.34)$$

In figure 2.6 the behaviour of angular momentum of a massive particle for different values of a against r_c is shown. It is noticed that once r_c approaches to r_{cmin} the value of the angular momentum goes to infinity. $\frac{r_c}{M} = 4$ (per unit mass M) is the only orbit in which the value of Rindler parameter does not matter and $\frac{L^2}{M^2} = 10$.

Substituting $\epsilon = 1$ in (2.30), gives energy of the massive particle

$$E^2 = \frac{4(a + \frac{u_c}{2} - Mu_c^2)^2}{u_c(a + u_c - 3Mu_c^2)}. \quad (2.35)$$

Figures 2.7, 2.8 and 2.9 show effective potential for massive particles for changing values of L with $a = 0$, $a = 0.01$ and $a = 2$. In figure 2.7, the graph to the right of the minimum points

is concave down while in figure 2.8 the graph to the right of the minimum points is steeply rising and concave up. In figure 2.7 for the given energy larger than the asymptotic value of effective potential, the particle would escape to infinity while with $a = 0.01$ and $a = 2$ the particle would fall into the singularity even if energy is bigger than the local maxima to the left of the minimum points.

Hence, massive particles have stable as well as unstable circular orbits. In figure 2.8 for $a = 0.01$ massive particles in the presence of Rindler acceleration have stable circular orbits at $r = 5.4$, $r = 6.8$, $r = 7.7$ and $r = 8.4$ with changing values of L^2 such as 14, 16, 18 and 20 respectively. Massive particles have unstable orbits at $r = 4.7$, $r = 4$, $r = 3.7$ and $r = 3.6$ with $L^2 = 14$, $L^2 = 16$, $L^2 = 18$ and $L^2 = 20$, respectively.

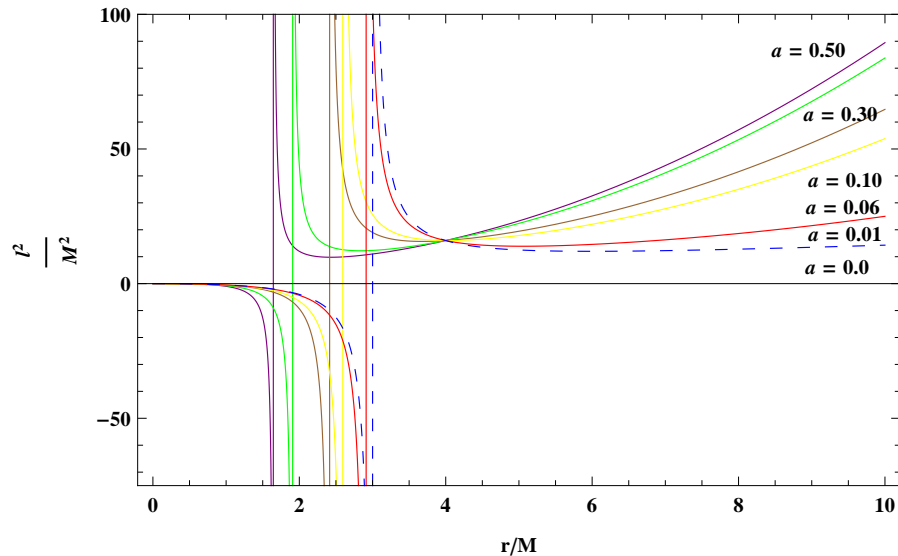


Figure 2.6: Angular momentum behaviour of a massive particle versus distance for changing a . It is observed that all curves coincide at $\frac{r_c}{M} = 4$.

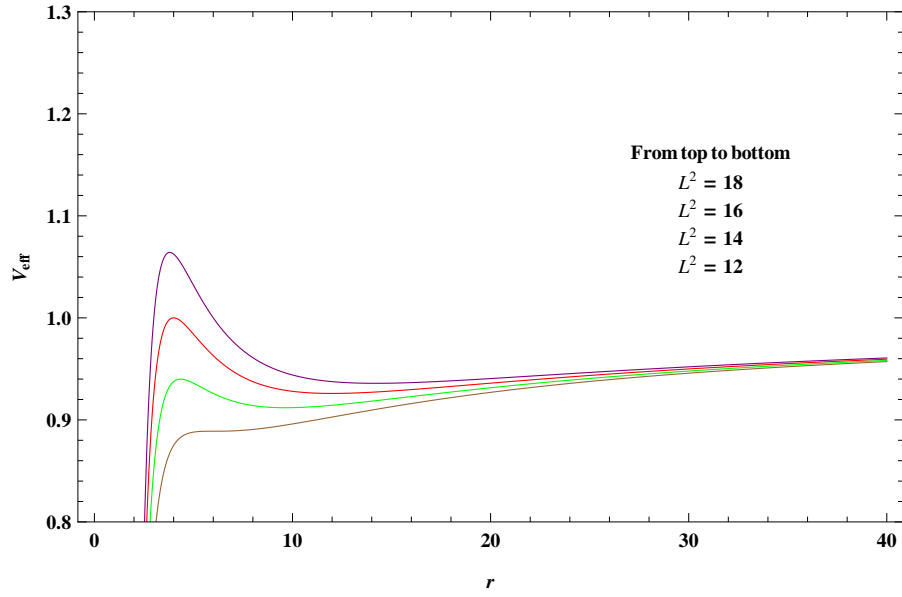


Figure 2.7: Effective potential for massive particle for changing L with $a = 0$.

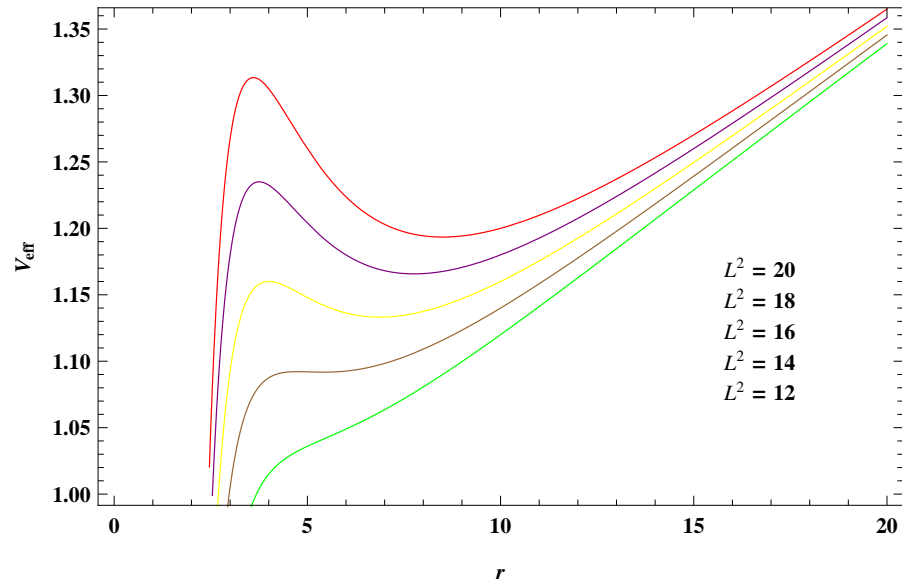


Figure 2.8: Effective potential for massive particle for changing L with $a = 0.01$.

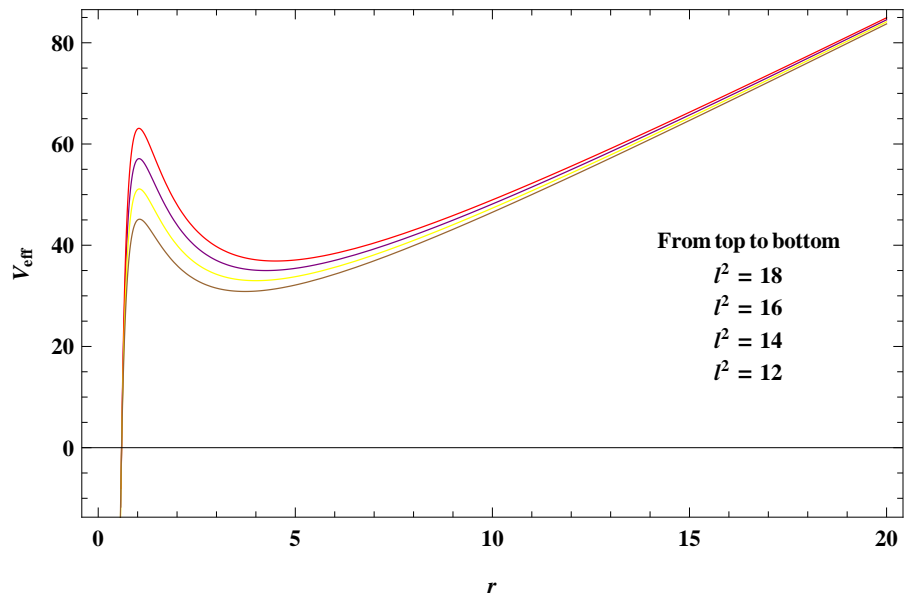


Figure 2.9: Effective potential for massive particle for changing L with $a = 2$.

Chapter 3

Motion of a Particle in the Spacetime Field of the Schwarzschild Black Hole with String Cloud Background

3.1 Introduction

The physical situation at the early stages of the formation of the universe was very complicated. During the initial stages of the development of the universe, phase transitions occurred that might have left traces that are still visible today. Phase transition led to symmetry breaking and thus the formation of topological defects. Topological defects can occur when the field symmetries are broken. Symmetry breaking happens when the universe cools down below some critical temperature and field is forced to choose a vacuum state [32].

Due to symmetry breaking, energy can get trapped in specific regions of space. The topological structure of this trapped energy determines the nature of the defect. A line-like defect is called *Cosmic String*. Besides cosmic strings, other defects can occur, such as domain walls and monopoles. With every broken symmetry there is a possibility for a topological defect, which could lead to the formation of cosmic strings.

Cosmic strings have some properties. There are many ways to detect the strings. Cosmic string creates a wedge in spacetime when it is formed during the one of the phase transitions. When light passes a string, light deformed due to the gravity exerted by the string. Hence, they may act as gravitational lenses. The lensing causes two exact similar objects to appear in the sky.

The second way of detecting a string is by measuring gravitational waves. Oscillating loops of strings generates gravitational wave background. They are capable of emitting gravitational radiations by forming cusps and kinks. This happens when strings intersects with themselves or each other. Both types of gravitational waves can be detected, but that depends on the tension of the string [32].

Cosmic string can cause density perturbations that eventually cause galaxy formation. A string moving through a region of dust will leave an over dense-accretion region behind it. Because there is an area cut out spacetime caused by the string the dust particles will eventually collide, resulting in an accretion disk in the string wake. This may give rise to the density fluctuations [33].

If string couple to other forces, cusps and kinks can emit beam of variety of forms of radiation which can potentially be detected on earth as cosmic rays. The gravitational coupling between photons and cosmic strings leads to emission of light from string.

The association of strings with black holes is suggested by the relationship between entropy of black hole horizon and string states [41]. A string cloud is a collection of strings that during the expansion of our universe have been intersecting with each other. So far no detection of a cosmic string has been reported but, strings are an interesting topic to study from theoretical point of view.

In this chapter, we will investigate the trajectories of the timelike and null geodesics for radial and circular motion in the Schwarzschild black hole with string cloud background. Here we consider a particle moving around a black hole in equatorial plane. We assume spherically symmetric metric on a non rotating black hole of mass M at rest. To achieve this, we first review the theory of a string cloud [34].

The action of the string evolving in the spacetime is

$$I_s = \int \mathcal{L} d\lambda^0 d\lambda^1, \quad (3.1)$$

where

$$\mathcal{L} = M\sqrt{-\gamma}, \quad (3.2)$$

and M is a positive constant that characterizes each string.

$$\gamma = \det\gamma_{AB}, \quad (3.3)$$

$$\gamma_{AB} = g_{\mu\nu} \frac{\partial x^\mu}{\partial \lambda^A} \frac{\partial x^\nu}{\partial \lambda^B}; \quad A, B = 0, 1. \quad (3.4)$$

Since string moves in two dimensions, it creates a world sheet in spacetime, equation (3.4) represents two dimensional world sheet metric. $x^\mu = x^\mu(\lambda^A)$ expresses the world sheet with parameter λ^0 for timelike and λ^1 for spacelike.

A bivector is an antisymmetric tensor of second rank. It is defined as [34]

$$\Sigma^{\mu\nu} = \epsilon^{AB} \frac{\partial x^\mu}{\partial \lambda^A} \frac{\partial x^\nu}{\partial \lambda^B}, \quad (3.5)$$

here ϵ^{AB} is the two dimensional Levi Civita symbol normalized as: $\epsilon^{01} = -\epsilon^{10} = 1$. So, the Lagrangian density can be written as

$$\mathcal{L} = \left(-\frac{1}{2} \Sigma^{\alpha\beta} \Sigma_{\alpha\beta} \right)^{\frac{1}{2}}. \quad (3.6)$$

The energy momentum tensor for a cloud of strings is

$$T^{\mu\nu} = \rho_0 \left(\Sigma^{\mu\beta} \Sigma_{\beta}{}^{\nu} \right) (-\gamma)^{-\frac{1}{2}}, \quad (3.7)$$

In mixed form we would find the general solution to EFEs for a cloud of strings in spherically symmetry. General static spherically symmetric metric is,

$$ds^2 = -e^{\nu(r)} dt^2 + e^{\lambda(r)} dr^2 + r^2 d\theta^2 + r^2 \sin^2 \theta d\phi^2, \quad (3.8)$$

here ν and λ are functions of r . The nonzero Christoffel symbols are as follow,

$$\begin{aligned} \Gamma^0{}_{10} &= \frac{\nu'}{2}, & \Gamma^1{}_{00} &= \frac{1}{2} \frac{e^\nu}{e^\lambda} \nu', & \Gamma^1{}_{22} &= -\frac{r}{e^\lambda}, \\ \Gamma^1{}_{11} &= \frac{\lambda'}{2} \lambda', & \Gamma^2{}_{12} &= \frac{1}{r}, & \Gamma^1{}_{33} &= -\frac{r \sin^2 \theta}{e^\lambda}, \\ \Gamma^3{}_{23} &= \frac{\cos \theta}{\sin \theta}, & \Gamma^3{}_{13} &= \frac{1}{r}, & \Gamma^2{}_{33} &= -\sin \theta \cos \theta. \end{aligned}$$

The surviving components of the Ricci tensors are

$$R_{00} = 2\nu'' + \nu'^2 - \nu' \lambda' + \frac{4\nu'}{r}. \quad (3.9)$$

$$R_{11} = 2\nu'' + \nu'^2 - \nu' \lambda' - \frac{4\lambda'}{r}. \quad (3.10)$$

$$R_{22} = e^{-\lambda} \left(1 + \frac{1}{2} r (\nu' - \lambda') \right) - 1, \quad (3.11)$$

As from [34]

$$\Sigma^{01} = \frac{\alpha}{\rho r^2} e^{-(\lambda+\nu)/2},$$

is the only non-zero component due to the spacetime symmetries so, only following components of energy-momentum tensor survive,

$$\begin{aligned} T^{00} &= \rho \Sigma^{01} \Sigma_1{}^0 (-\gamma)^{-\frac{1}{2}}, \\ T^{00} &= e^{-\nu} \frac{\alpha}{r^2}, \end{aligned}$$

Similarly,

$$\begin{aligned} T_{00} &= \frac{\alpha}{r^2} e^\nu, \\ T^0{}_0 = T^1{}_1 &= \frac{\alpha}{r^2}, \end{aligned}$$

Using the value of Ricci tensor, Ricci scalar and stress-energy-momentum tensor, in the EFEs for the clouds

$$\begin{aligned} R_{00} &= \frac{1}{2} g_{00} R - T_{00}, \\ R_{00} &= \frac{1}{2} e^\nu \left(\frac{2\alpha}{r^2} \right) - \frac{\alpha}{r^2} e^\nu, \end{aligned}$$

i.e

$$R_{00} = 0. \quad (3.12)$$

$$\begin{aligned} R_{11} &= \frac{1}{2} g_{11} R - T_{11} \\ R_{11} &= -\frac{1}{2} e^\lambda \left(\frac{2\alpha}{r^2} \right) + \frac{\alpha}{r^2} e^\lambda, \\ R_{11} &= 0. \end{aligned} \quad (3.13)$$

$$\begin{aligned} R_{22} &= \frac{1}{2} g_{22} R - T_{22} \\ R_{22} &= -\frac{1}{2} r^2 \left(\frac{2\alpha}{r^2} \right), \end{aligned}$$

$$R_{22} = -\alpha. \quad (3.14)$$

from equations (3.9),(3.10),(3.11),(3.12),(3.13) and (3.14),

$$2\nu'' + \nu'^2 - \nu'\lambda' + \frac{4\nu'}{r} = 0, \quad (3.15)$$

$$2\nu'' + \nu'^2 - \nu'\lambda' - \frac{4\lambda'}{r} = 0, \quad (3.16)$$

$$e^{-\lambda}\left(1 + \frac{1}{2}r(\nu' - \lambda')\right) - 1 = -\alpha, \quad (3.17)$$

Subtracting (3.15) from (3.16),

$$\frac{4\nu'}{r} + \frac{4\lambda'}{r} = 0,$$

$$\nu' + \lambda' = 0,$$

$$\nu = -\lambda, \quad (3.18)$$

Using (3.18) in (3.17),

$$e^{-\lambda}\left(1 + \frac{1}{2}r(-\lambda' - \lambda')\right) - 1 = -\alpha,$$

$$e^{-\lambda}\left(1 + \frac{2r\lambda'}{2}\right) - 1 = -\alpha,$$

$$(e^{-\lambda}r)' = 1 - \alpha,$$

$$(e^{-\lambda}r) = r - \alpha r + \beta,$$

where β is the constant of integration

$$e^{-\lambda} = 1 - \alpha + \frac{\beta}{r},$$

Considering the weak field limit we can identify β as follows. If the gravitational source is spherically symmetric having mass M than in the weak field limit we have $g_{00} = 1 + \frac{2\Phi}{c^2}$, where $\Phi = \frac{-GM}{r}$ is Newtonian potential. So, [9]

$$\beta = -2M$$

Substituting the value of β , (3.8) implies

$$ds^2 = -\left(1 - \frac{2M}{r} - \alpha\right)dt^2 + \left(1 - \frac{2M}{r} - \alpha\right)^{-1}dr^2 + r^2d\theta^2 + r^2\sin^2\theta d\phi^2. \quad (3.19)$$

This solution was first obtained by Letelier [34] and the metric (3.19) represents the black hole spacetime associated with a spherical mass M centered at the origin of the system of coordinates, surrounded by a spherical cloud of strings. Here M is the mass of the black hole and α is string cloud parameter, M is not a function of α . For the realistic model string cloud parameter is restricted to $0 < \alpha < 1$ [35]. The cloud of strings with no central mass have no horizons, it has naked singularity at $r = 0$. It is recovered that with $\alpha = 0$ (3.19) reduces to Schwarzschild case. The horizon of (3.19) is given by

$$1 - \frac{2M}{r} - \alpha = 0, \\ r_h = \frac{2M}{1 - \alpha}, \quad \alpha \in (0, 1). \quad (3.20)$$

If $\alpha < 1$ than the radius is larger than the Schwarzschild radius by the amount $(1 - \alpha)^{-1}$. In the limit $\alpha \rightarrow 0$ in (3.20) we have Schwarzschild radius, and $\alpha \rightarrow 1$ implies radius of the event horizon tends to infinity. We will investigate trajectories of the timelike and null geodesics for radial and circular motion in the above spacetime given by metric (3.19).

3.2 Particle Trajectories

For the spacetime given by (3.19) the geodesic Lagrangian for particle is given by

$$\mathcal{L} = \frac{m}{2}g_{\mu\nu}\dot{x}^\mu\dot{x}^\nu = m\left(-\frac{1}{2}\left(1 - \frac{2M}{r} - \alpha\right)\dot{t}^2 + \frac{\dot{r}^2}{2\left(1 - \frac{2M}{r} - \alpha\right)} + \frac{1}{2}r^2(\dot{\theta}^2 + \sin^2\theta\dot{\phi}^2)\right). \quad (3.21)$$

Using the Euler-Lagrange equations we get

$$-\left(1 - \frac{2M}{r} - \alpha\right)\dot{t} = \text{constant} = \frac{\varepsilon}{m} = E$$

$$\dot{t} = \frac{-\epsilon}{\left(1 - \frac{2M}{r} - \alpha\right)m} = \frac{-E}{\left(1 - \frac{2M}{r} - \alpha\right)}. \quad (3.22)$$

And

$$2\dot{\phi}r^2 \sin^2 \theta = \text{constant},$$

$$\dot{\phi}r^2 \sin^2 \theta = \text{constant} = \frac{l}{m} = L. \quad (3.23)$$

For massless particles, E is the conserved energy and L is an angular momentum, while for massive particles they are the conserved energy and angular momentum per unit mass of the particle. In the equatorial plane, we get $L = r^2\dot{\phi}$

In the equatorial plane (2.8) implies

$$-\left(1 - \frac{2M}{r} - \alpha\right)\dot{t}^2 + \frac{\dot{r}^2}{\left(1 - \frac{2M}{r} - \alpha\right)} + r^2\dot{\phi}^2 = -\epsilon.$$

Using (3.22) and (3.23) in above equation we get

$$-\frac{\left(1 - \frac{2M}{r} - \alpha\right)E^2}{\left(1 - \frac{2M}{r} - \alpha\right)^2} + \frac{\dot{r}^2}{\left(1 - \frac{2M}{r} - \alpha\right)} + r^2\frac{L^2}{r^4} = -\epsilon,$$

$$\left(\frac{dr}{d\lambda}\right)^2 = E^2 - \left(1 - \frac{2M}{r} - \alpha\right)\left(\epsilon + \frac{L^2}{r^2}\right), \quad (3.24)$$

$$\frac{1}{2}\left(\frac{dr}{d\lambda}\right)^2 + V_{eff}(r) = \frac{1}{2}E^2. \quad (3.25)$$

Here $V_{eff}(r) = \frac{1}{2}\left(1 - \frac{2M}{r} - \alpha\right)\left(\epsilon + \frac{L^2}{r^2}\right)$ is the effective potential and the corresponding effective energy is

$$E_{eff} = \frac{1}{2}E^2.$$

The potential of a particle in Schwarzschild spacetime with string cloud background is decreasing with the increasing value of string cloud parameter when compared with Schwarzschild case.

3.3 Radial Motion

In the case of radial motion ϕ is constant and $L = 0$. Hence, (3.24) implies

$$\left(\frac{dr}{d\lambda}\right)^2 = E^2 - \epsilon\left(1 - \frac{2M}{r} - \alpha\right). \quad (3.26)$$

3.3.1 Null Geodesics

In null geodesics, which refers to the motion of massless particles. For massless particles we can choose any affine parameter along the null geodesic. So, (3.26) becomes

$$\left(\frac{dr}{d\lambda}\right)^2 = E^2. \quad (3.27)$$

Using (3.22) in (3.27)

$$\begin{aligned} \left(\frac{dr}{d\lambda}\right)^2 &= \left(-\left(1 - \frac{2M}{r} - \alpha\right)\frac{dt}{d\lambda}\right)^2, \\ \frac{dr}{dt} &= \pm\left(1 - \frac{2M}{r} - \alpha\right), \end{aligned}$$

On integrating we have

$$\begin{aligned} t &= \frac{r - r\alpha + 2M \ln \left[\frac{2M}{r} + (\alpha - 1) \right]}{(\alpha - 1)^2}, & (\text{Outgoing photon}) \\ t &= \frac{-r + r\alpha - 2M \ln \left[\frac{2M}{r} + (\alpha - 1) \right]}{(\alpha - 1)^2}, & (\text{Ingoing photon}) \end{aligned}$$

The photons worldlines will have slopes $\pm(1 - \alpha)$ as $r \rightarrow \infty$, but their slopes approaches $\pm\infty$ as $r \rightarrow \frac{2M}{1-\alpha}$. This means the lightcone expands if $r \rightarrow \infty$ as compared to Schwarzschild case and the lightcone become more vertical, it closes up, as $r \rightarrow \frac{2M}{1-\alpha}$. Thus, the particle reaches $r = \frac{2M}{1-\alpha}$ when $t \rightarrow \infty$. For an external observer the particle take an infinite time to reach the horizon.

3.3.2 Timelike Geodesics

We are considering timelike geodesics we can choose our affine parameter to be the proper time τ along the trajectory. With unit mass (3.26) becomes

$$\left(\frac{dr}{d\tau}\right)^2 = E^2 - \left(1 - \frac{2M}{r} - \alpha\right), \quad (3.28)$$

Now first we find the equation of motion by using Euler-Lagrange equation (2.16). Consider (3.21) in equatorial plane and differentiate with respect to r and \dot{r} ,

$$\frac{\partial \mathcal{L}}{\partial r} = \left(\frac{-M}{r^2}\right)\dot{t}^2 - \frac{1}{\left(1 - \frac{2M}{r} - \alpha\right)^2} \left(\frac{M}{r^2}\right)\dot{r}^2, \quad (3.29)$$

$$\frac{\partial \mathcal{L}}{\partial \dot{r}} = \frac{\dot{r}}{\left(1 - \frac{2M}{r} - \alpha\right)},$$

$$\frac{d}{d\tau} \left(\frac{\partial \mathcal{L}}{\partial \dot{r}}\right) = \frac{\left(1 - \frac{2M}{r} - \alpha\right)\ddot{r} - \dot{r}^2 \left(\frac{2M}{r^2}\right)}{\left(1 - \frac{2M}{r} - \alpha\right)^2}, \quad (3.30)$$

Now using (3.29) and (3.30) in Euler Lagrange equation, we get

$$\frac{\ddot{r}}{\left(1 - \frac{2M}{r} - \alpha\right)} - \frac{\dot{r}^2 \left(\frac{2M}{r^2}\right)}{\left(1 - \frac{2M}{r} - \alpha\right)^2} + \left(\frac{M}{r^2}\right)\dot{t}^2 - r\dot{\phi}^2 = 0. \quad (3.31)$$

Here for the radial motion (3.31) becomes

$$\frac{\ddot{r}}{\left(1 - \frac{2M}{r} - \alpha\right)} - \frac{\dot{r}^2 \left(\frac{M}{r^2}\right)}{\left(1 - \frac{2M}{r} - \alpha\right)^2} + \left(\frac{M}{r^2}\right)\dot{t}^2 = 0. \quad (3.32)$$

Inserting (3.28) and (3.22) in (3.32), we obtain

$$\frac{\ddot{r}}{\left(1 - \frac{2M}{r} - \alpha\right)} - \frac{\left(E^2 - \left(1 - \frac{2M}{r} - \alpha\right)\right) \left(\frac{M}{r^2}\right)}{\left(1 - \frac{2M}{r} - \alpha\right)^2} + \frac{\left(\frac{M}{r^2}\right)}{\left(1 - \frac{2M}{r} - \alpha\right)^2} E^2 = 0,$$

$$\ddot{r} = \frac{d^2 r}{d\tau^2} = -\frac{M}{r^2}. \quad (3.33)$$

In above equation there is no contribution of string cloud parameter, this is same as corresponding equation of motion in Schwarzschild case. But this does not implies that in both theories particle predicts the same physical behaviour. Here, r coordinate is the radial distance, the dot indicates derivative with respect to proper time rather than coordinate time. As a specific example consider the particle initially at rest and, upon the gravitational attraction, starts moving from its radial location $r = r_0$ using

$$\begin{aligned} \left(\frac{dr_0}{d\tau}\right)^2 &= E^2 - 1 + \frac{2M}{r_0} + \alpha, \\ 0 &= E^2 - 1 + \frac{2M}{r_0} + \alpha, \\ E^2 &= 1 - \frac{2M}{r_0} - \alpha, \\ \left(\frac{dr}{d\tau}\right)^2 &= E^2 - 1 + \frac{2M}{r} + \alpha, \end{aligned} \tag{3.34}$$

Substituting (3.34) in the above equation, we obtain

$$\left(\frac{dr}{d\tau}\right)^2 = 2M\left(\frac{1}{r} - \frac{1}{r_0}\right). \tag{3.35}$$

Above equation has the same form as the Schwarzschild case equating the gain in kinetic energy to the loss in gravitational potential energy for a particle falling from rest at $r = r_0$. Consider a particle dropped from rest at infinity. In this case setting $E = 1$ in the geodesic equation (3.22) and in (3.28) we obtain

$$\begin{aligned} \frac{dt}{d\tau} &= \frac{1}{-(1 - \frac{2M}{r} - \alpha)}, \\ \frac{dr}{d\tau} &= \sqrt{\frac{2M}{r} + \alpha}, \end{aligned} \tag{3.36}$$

From these equations the components of the four-velocity of the particle in its radial motion in equatorial plane are

$$\frac{dx^\mu}{d\tau} = \left(\frac{1}{-(1 - \frac{2M}{r} - \alpha)}, \sqrt{\frac{2M}{r} + \alpha}, 0, 0 \right).$$

Equation (3.36) determines the trajectory of $r(\tau)$, integrating (3.36) gives

$$\tau = \frac{r\sqrt{\frac{2M}{r} + \alpha} + r_0\sqrt{\frac{2M}{r_0} + \alpha}}{\alpha} - \frac{\left[M \ln \left(\frac{M}{r} + \alpha + \sqrt{\alpha}\sqrt{\frac{2M}{r} + \alpha} \right) \left(\frac{M}{r_0} + \alpha + \sqrt{\alpha}\sqrt{\frac{2M}{r_0} + \alpha} \right) \right]}{\alpha^{\frac{2}{3}}}$$

where $\tau = 0$ at $r = r_0$. Here τ is the proper time of the particle falling from $r = r_0$ to a coordinate radius r . For any value of string cloud parameter particle takes a finite proper time to reach $r = 0$. From (3.25) effective potential for massive particles in radial motion is

$$V_{eff}(r) = \frac{1}{2} \left(1 - \frac{2M}{r} - \alpha \right). \quad (3.37)$$

In figure 3.1 effective potential V_{eff} for different values of α against $\frac{r}{M}$ (for unit mass M) is plotted. This shows that the effective potential decreases with the increasing value of string cloud parameter α . Here the horizon r_h is the intersection of V_{eff} with $\frac{r}{M}$ axis. Event horizons are 2.2, 3.3, 4, 5, 20 for $\alpha = 0.1, 0.4, 0.5, 0.6, 0.9$ respectively.

Substituting (3.22) in (3.28), we have

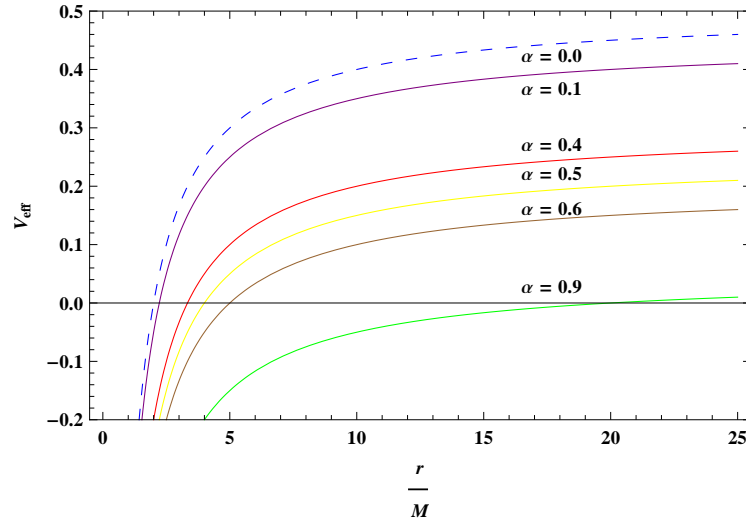


Figure 3.1: Plot of V_{eff} in terms of $\frac{r}{M}$. The effective potential decreases with the increasing α . Eq.(3.37) $\frac{r}{M}$ (for unit mass M) ranges from 0 to 20.

$$\begin{aligned}\left(\frac{dr}{d\tau}\right)^2 &= \left(1 - \frac{2M}{r} - \alpha\right)^2 \left(\frac{dt}{d\tau}\right)^2 - 1 + \frac{2M}{r} + \alpha, \\ \frac{\left(\frac{dr}{d\tau}\right)^2}{\left(\frac{dt}{d\tau}\right)^2} &= \frac{\left(1 - \frac{2M}{r} - \alpha\right)^2 \left(\frac{dt}{d\tau}\right)^2}{\left(\frac{dt}{d\tau}\right)^2} + \frac{-1 + \frac{2M}{r} + \alpha}{\left(\frac{dt}{d\tau}\right)^2}.\end{aligned}$$

This yields

$$\left(\frac{dr}{dt}\right)^2 = \frac{1}{E^2} \left(E^2 - 1 + \frac{2M}{r} + \alpha\right) \left(1 - \frac{2M}{r} - \alpha\right)^2,$$

On integrating, we get

$$\begin{aligned}\pm(t - t_0) &= - \frac{\sqrt{-1 + \alpha + E^2 + \frac{2M}{r}} \left[\frac{(\alpha-1) \frac{r}{M} \sqrt{-1 + \alpha + E^2 + \frac{2M}{r}}}{\alpha-1 + E^2} \right]}{(\alpha - 1)^2 \sqrt{\frac{-1 + \alpha + E^2 + \frac{2M}{r}}{E^2}}} \\ &\quad + \frac{\frac{2 \ln[2 + (\alpha-1) \frac{r}{M}]}{E} - \frac{2 \ln[2 + (\alpha-1 + 2E^2 - 2E \sqrt{-1 + \alpha + E^2 + \frac{2M}{r}}) \frac{r}{M}]}{E}}{(\alpha - 1)^2 \sqrt{\frac{-1 + \alpha + E^2 + \frac{2M}{r}}{E^2}}}.\end{aligned}$$

Here t is the coordinate time experienced by stationary distant observer. We can conclude that to such an observer, it takes an infinite time for the particle to reach $r = \frac{2M}{1-\alpha}$, we note that $t \rightarrow \infty$ as $r \rightarrow \frac{2M}{1-\alpha}$. From figure 3.2 it is observed that the string cloud parameter accelerates the particles following the timelike geodesics so that the particles reach the horizon faster than the Schwarzschild case ($\alpha = 0$). It is clear from figure 3.2 that as the value of α increases, the particles take less time to reach the horizon. In figure 3.3 and 3.4 singularity versus coordinate time in string cloud background is compared with Schwarzschild case.

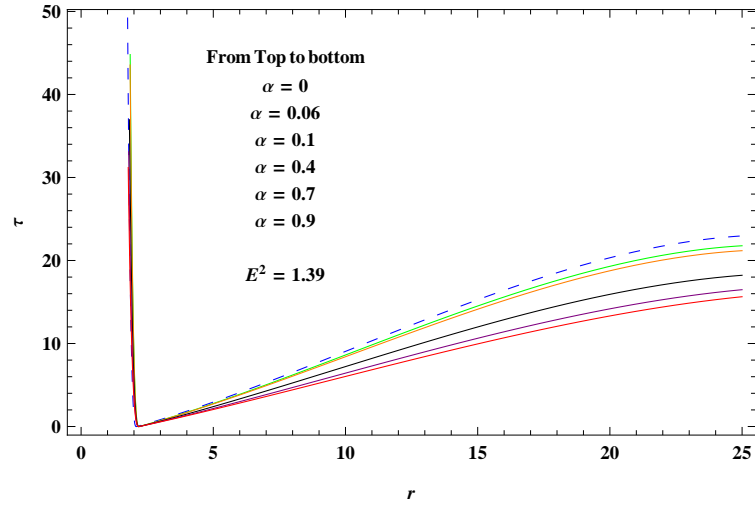


Figure 3.2: Plot of singularity versus proper time. The fall delays in Schwarzschild case compared to string cloud background case.

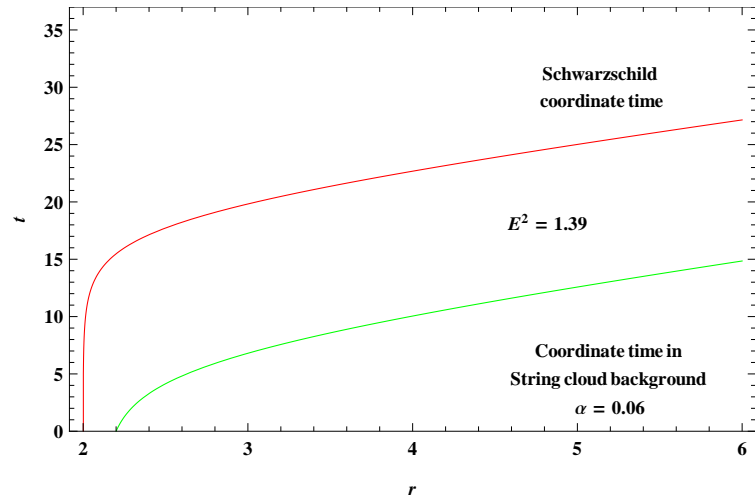


Figure 3.3: Plot of singularity versus coordinate time in Schwarzschild case and in string cloud background.

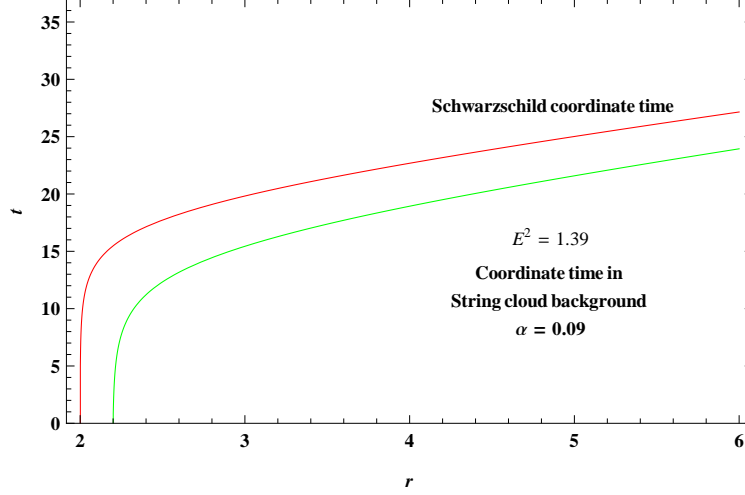


Figure 3.4: Plot of singularity versus coordinate time in schwarzschild case and in string cloud background.

3.4 Circular Motion

In this section we would study the circular motion of a photon and a massive particle. For circular motion in equatorial plane we have $r = \text{constant}$, which implies $\dot{r} = \ddot{r} = 0$. As before, we introduce $r = \frac{1}{u}$. By considering $\frac{du}{d\phi}$ at $u = u_c$ is zero in which $r_c = \frac{1}{u_c}$ is the circular orbit of the particle.

Using chain rule

$$\dot{r} = \frac{dr}{d\sigma} = \frac{dr}{d\phi} \frac{d\phi}{d\sigma} = \frac{dr}{d\phi} \frac{L}{r^2},$$

(3.24) becomes

$$\left(\frac{du}{d\phi}\right)^2 = \frac{E^2}{L^2} - \left(1 - 2Mu - \alpha\right) \left(\frac{\epsilon}{L^2} + u^2\right). \quad (3.38)$$

$$\left(\frac{du}{d\phi}\right)^2 = \frac{E^2}{L^2} - \frac{\epsilon}{L^2} - u^2 + \frac{2M\epsilon u}{L^2} + 2Mu^3 + \frac{\alpha\epsilon}{L^2} + \alpha u^2.$$

Taking derivative of both sides with respect to ϕ

$$\frac{d^2u}{d\phi^2} = -u + \frac{M\epsilon}{L^2} + 3Mu^2 + \alpha u.$$

At $u = u_c$

$$\frac{E^2}{L^2} - \left(1 - 2Mu_c - \alpha\right) \left(\frac{\epsilon}{L^2} + u_c^2\right) = 0. \quad (3.39)$$

In the circular motion we have $\frac{d^2u}{d\phi^2} = 0$, therefore for (3.39)

$$\frac{d}{du} \left[\left(\frac{E^2}{L^2} - \left(1 - 2Mu + \frac{2\alpha}{u} \left(\frac{\epsilon}{L^2} + u^2 \right) \right) \right) \right]_{u=u_c} = 0. \quad (3.40)$$

These conditions give the expression for the angular momentum.

$$-u_c + \frac{M\epsilon}{L^2} + 3Mu_c^2 + \alpha u_c = 0,$$

solving for L^2 gives

$$L^2 = \frac{M\epsilon}{u_c(1 - \alpha - 3Mu_c)}. \quad (3.41)$$

Energy of the particle: Substituting (3.41) in (3.39)

$$\frac{E^2}{L^2} - \epsilon \left(\frac{u_c(1 - \alpha - 3Mu_c)}{M\epsilon} \right) - u_c^2 + 2M\epsilon u_c \left(\frac{u_c(1 - \alpha - 3Mu_c)}{M\epsilon} \right)$$

solving for E^2 gives,

$$E^2 = \frac{\epsilon(\alpha + 2Mu_c - 1)^2}{(1 - \alpha - 3Mu_c)}. \quad (3.42)$$

For physically acceptable motion of the particle $1 - \alpha - 3Mu_c$ must be greater than zero, this constraint arises from (3.41) and

$$r_c - \alpha r_c - 3M > 0,$$

$$r_c > \frac{3M}{1 - \alpha} = r_{cmin}.$$

Here r_{cmin} is larger than the horizon

$$r_h = \frac{2M}{1 - \alpha}, \quad \alpha \in (0, 1)$$

Hence, the geodesic equation $r^2\dot{\phi} = L$ cannot be satisfied for circular orbits with $r < \frac{3M}{1 - \alpha}$. Since they do not satisfy the geodesics equation so these orbits are not geodesics and cannot followed by freely falling particles. Thus, the circular orbit cannot be maintained by a free massive particle with $r < \frac{3M}{1 - \alpha}$ around spherical massive body.

3.4.1 Null Geodesics

For massless particle geodesics (3.41) shows that only possible radius for circular photon orbit is

$$\alpha r_c - r_c + 3M = 0,$$

which gives

$$r_c = \frac{3M}{1 - \alpha}. \quad (3.43)$$

In figure 3.5 we plot $\frac{r_c}{M}$ versus αM from (3.43) (for unit mass M). This shows that for larger value of string cloud parameter α , the circular orbit of photon has larger radius. In this case

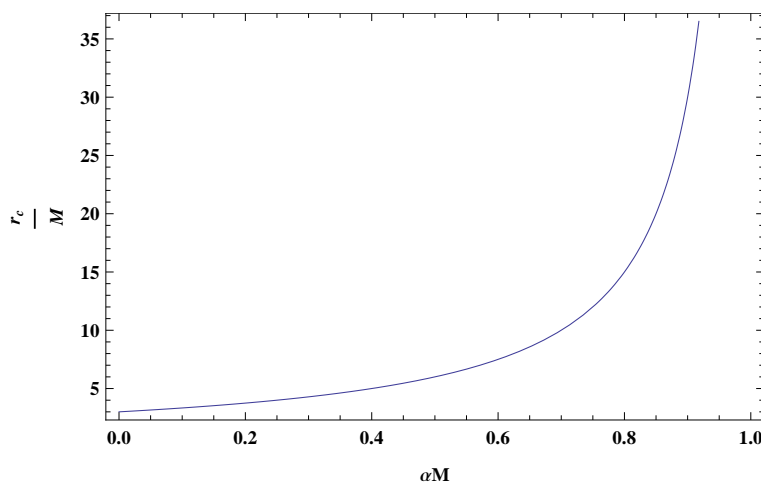


Figure 3.5: Plot of $\frac{r_c}{M}$ in terms of αM for a massless particle. For larger value of α the circular orbit of photon has larger radius.

from (3.39)

$$\begin{aligned} \frac{E^2}{L^2} &= (1 - 2Mu_c - \alpha)(u_c^2), \\ \frac{E^2}{L^2} &= \left(\frac{1 - \alpha}{3M}\right)^2 - 2M\left(\frac{1 - \alpha}{3M}\right)^3 - \alpha\left(\frac{1 - \alpha}{3M}\right)^2, \end{aligned}$$

after simplification

$$\frac{E^2}{L^2} = \frac{(1 - \alpha)^3}{27M^2}. \quad (3.44)$$

Having r_c known, an exact value for the specific value of M and α means that for photon

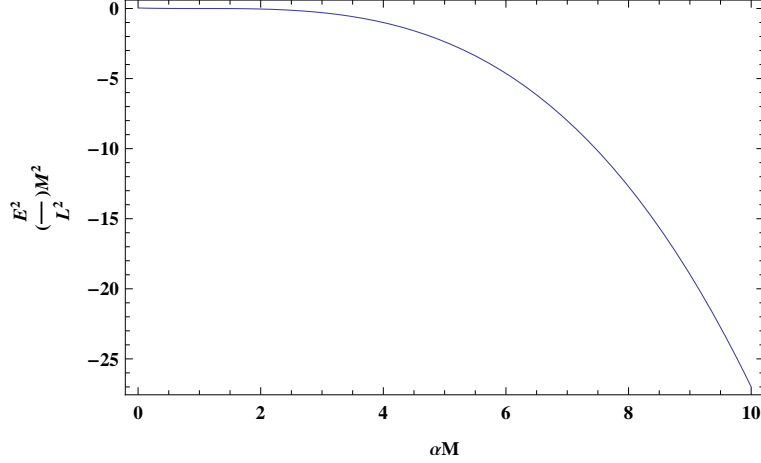


Figure 3.6: Plot of $\frac{E^2}{L^2}(M^2)$ in terms of αM for a massless particle. For larger value of α the circular orbit of photon has smaller value of $\frac{E^2}{L^2}$ (3.44).

there exist only one equilibrium circular orbit with the ratio $\frac{E^2}{L^2}$. From (3.44) the plot of $(\frac{E^2}{L^2})M^2$ against αM (for unit mass M) for a massless particle is shown in figure 3.6. For larger value of α the circular orbit of photon has smaller value of $(\frac{E^2}{L^2})M^2$.

Stability: Consider the geodesic equation of the photon in (3.24) and the replacement of $\tau = \frac{\tilde{r}}{L}$ gives

$$\left(\frac{dr}{d\tilde{r}}\right)^2 + V_{eff}(r) = E_{eff}(r),$$

where

$$V_{eff}(r) = \frac{\left(1 - \frac{2M}{r} - \alpha\right)}{r^2} = \frac{1 - \frac{2M}{r} - \alpha}{r^2}. \quad (3.45)$$

$$E_{eff}(r) = \frac{E^2}{L^2}.$$

For stable circular orbit we must have $V'_{eff} = 0$ at r_c and $V''_{eff} > 0$ at r_c

$$V''_{eff} = \frac{6}{r_c^4} - \frac{24M}{r_c^5} - \frac{6\alpha}{r_c^4},$$

$$V_{eff}'' = 6\left(\frac{1-\alpha}{3M}\right)^4 - 24M\left(\frac{1-\alpha}{3M}\right)^5 - 6\alpha\left(\frac{1-\alpha}{3M}\right)^4. \quad (3.46)$$

Considering unit mass M , and for $\alpha = 0.1$, (3.46) becomes,

$$V_{eff}'' = -0.01458.$$

For $\alpha = 0.5$, (3.46) becomes,

$$V_{eff}'' = -0.0007716.$$

For $\alpha = 0.9$, (3.46) becomes,

$$V_{eff}'' = -0.00000025.$$

Hence, V_{eff}'' is negative for $\alpha = 0.1$ to 0.9 so there is no stable circular orbit for photons.

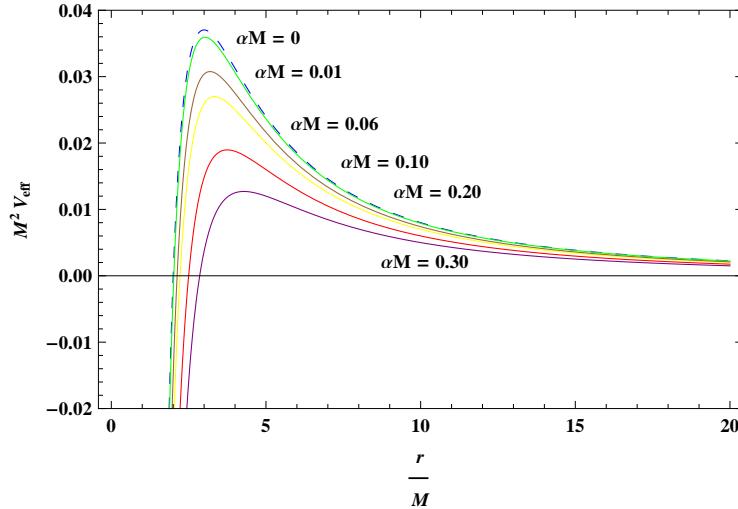


Figure 3.7: The plot $M^2 V_{eff}$ versus $\frac{r}{M}$ for photons shows the unstable circular orbits for photons.

Circular orbits will be stable if they corresponds to a minimum of the potential and, unstable if they corresponds to a maximum. We have plotted V_{eff} in figure 3.7 showing for different values of string cloud parameter there is no stable circular orbit for photons. This means that photon can orbit forever in this radius where V_{eff} is maximum, but any perturbation can cause it to fly away either to infinity or drop in singularity.

3.4.2 Timelike Geodesics

For timelike geodesics we set $\epsilon = 1$ in (3.41) to get the angular momentum

$$L^2 = \frac{M}{u_c(1 - \alpha - 3Mu_c)}. \quad (3.47)$$

and from (3.42) we have the energy of the particle

$$E^2 = \frac{(\alpha + 2Mu_c - 1)^2}{(1 - \alpha - 3Mu_c)}. \quad (3.48)$$

As this is mentioned before here $r_c = \frac{1}{u_c}$, from (3.47) figure 3.8 and 3.9 shows the variation of

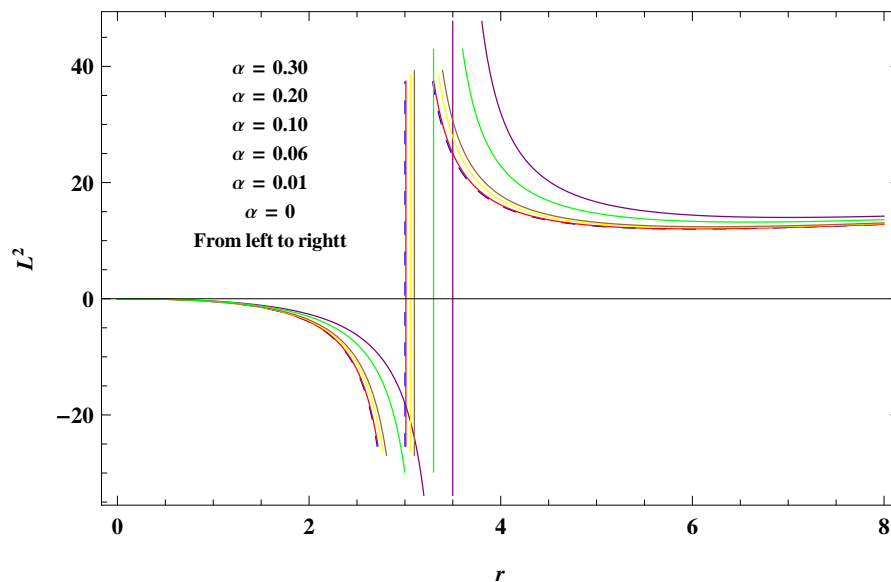


Figure 3.8: Behaviour of the angular momentum of massive particle versus distance for changing α . Here r ranges from 0 to 8.

L^2 against r_c . If the radius of circular orbit becomes smaller the angular momentum increases but when the value of radius of circular orbit approaches to r_{cmin} , the angular momentum goes to infinity.

For physical acceptable motion the constraints $(1 - \alpha - 3Mu_c) > 0$ arises from (3.47) which

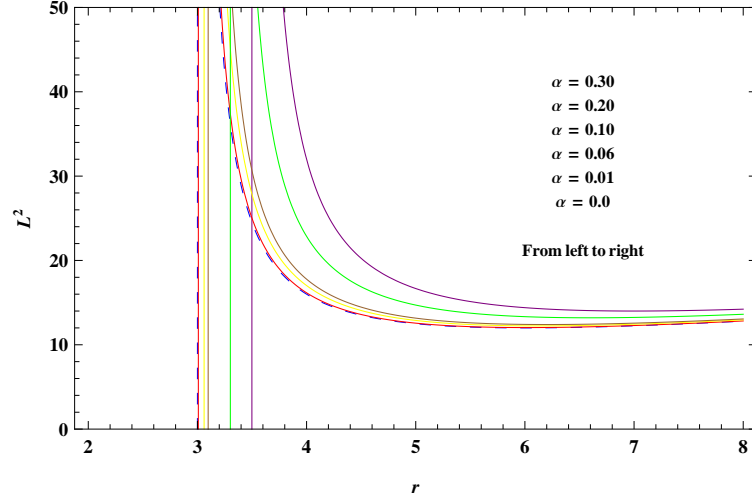


Figure 3.9: Behaviour of the angular momentum of massive particle versus distance for changing α . Here r ranges from 2 to 8.

implies $r_c > \frac{3M}{1-\alpha} = r_{cmin}$. Hence, $r_{cmin} - r_c = \frac{1}{1-\alpha}$. In figure 3.10 and 3.11 the difference between circular geodesic radii and horizon radii is shown, this shows that with larger value of string cloud parameter, the gap between r_{cmin} and r_h increases. Hence, when the value of string cloud parameter approaches to unity, the circular geodesic radii becomes unbounded and particle can escape to infinity.

Stability: Consider the geodesic equation (3.24), putting $\epsilon = 1$ in (3.24)

$$\left(\frac{dr}{d\tau}\right)^2 = E^2 - \left(1 - \frac{2M}{r} - \alpha\right)\left(\epsilon + \frac{L^2}{r^2}\right),$$

$$\frac{1}{L^2}\left(\frac{dr}{d\tau}\right)^2 = \frac{E^2}{L^2} - \left(1 - \frac{2M}{r} - \alpha\right)\left(\frac{\epsilon}{L^2} + \frac{1}{r^2}\right),$$

replacement of $\tau = \frac{\tilde{\tau}}{L}$ gives

$$\left(\frac{dr}{d\tilde{\tau}}\right)^2 + V_{eff}(r) = E_{eff}(r),$$

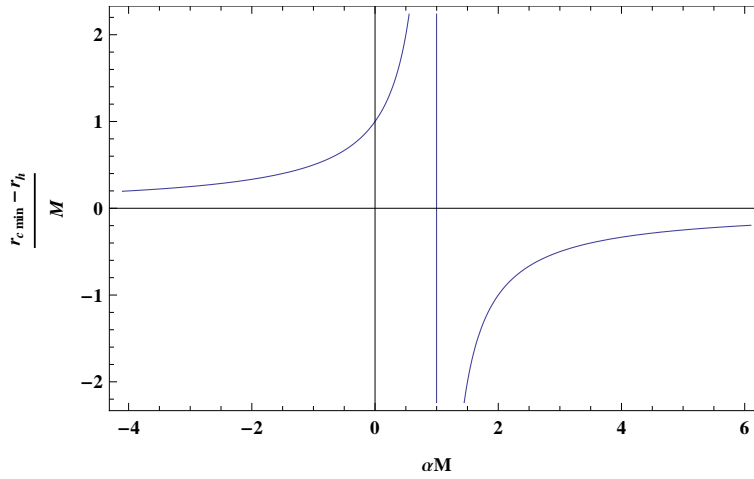


Figure 3.10: The difference between circular geodesic radii and horizon radii shown as αM

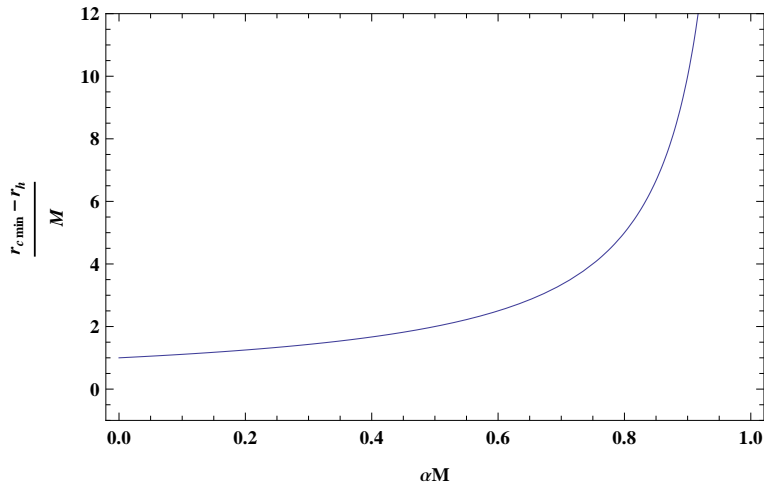


Figure 3.11: The difference between circular geodesic radii and horizon radii shown as αM

here

$$V_{eff}(r) = \left(1 - \frac{2M}{r} - \alpha\right) \left(\frac{\epsilon}{L^2} + \frac{1}{r^2}\right).$$

$$E_{eff}(r) = \frac{E^2}{L^2}.$$

As mentioned before for stable circular orbit we must have $V'_{eff} = 0$ and $V''_{eff} > 0$ at r_c

$$\begin{aligned} V_{eff} &= \left(1 - \frac{2M}{r} - \alpha\right) \left(\frac{1}{L^2} + \frac{1}{r^2}\right), \\ V_{eff} &= \frac{1}{L^2} + \frac{1}{r^2} - \frac{2M}{r^3} - \frac{\alpha}{r^2} - \frac{\alpha}{L^2} - \frac{2M}{L^2 r}, \\ V'_{eff} &= -\frac{2}{r^3} + \frac{6M}{r^4} + \frac{2\alpha}{r^3} + \frac{2M}{L^2 r^2}, \\ V''_{eff} &= \frac{6}{r_c^4} - \frac{24M}{r_c^5} - \frac{6\alpha}{r_c^4} - \frac{4M}{L^2 r_c^4}, \end{aligned}$$

putting $V'_{eff} = 0$, gives

$$\begin{aligned} r_{c1} &= \frac{(\alpha - 1)L^2 + \sqrt{(\alpha - 1)^2 L^4 - 12M^2 L^2}}{2M}, \\ r_{c2} &= \frac{(\alpha - 1)L^2 - \sqrt{(\alpha - 1)^2 L^4 - 12M^2 L^2}}{2M}. \end{aligned}$$

Substituting the value of r_c in V''_{eff}

$$\begin{aligned} V''_{eff} &= 6 \left(\frac{(\alpha - 1)L^2 \pm \sqrt{(\alpha - 1)^2 L^4 - 12M^2 L^2}}{2M} \right)^4 \\ &\quad - 24M \left(\frac{(\alpha - 1)L^2 \pm \sqrt{(\alpha - 1)^2 L^4 - 12M^2 L^2}}{2M} \right)^5 \\ &\quad - 6\alpha \left(\frac{(\alpha - 1)L^2 \pm \sqrt{(\alpha - 1)^2 L^4 - 12M^2 L^2}}{2M} \right)^4 \\ &\quad - \frac{4M\epsilon}{L^2} \left(\frac{(\alpha - 1)L^2 \pm \sqrt{(\alpha - 1)^2 L^4 - 12M^2 L^2}}{2M} \right)^4. \end{aligned}$$

Effective potential has maxima and minima for different values of r_c . Effective potential for $\alpha = 0.01$, $\alpha = 0.1$, and $\alpha = 0.25$ is shown in figures 3.12, 3.13, and 3.14 respectively. There are five different curves depending on the angular momentum. In figure 3.12 graph of effective potential for $\alpha = 0.01$ gives the maximum value at $r = 4.4$, $r = 4.0$, $r = 3.8$ and $r = 3.7$, minimum value at $r = 9.3$, $r = 11.7$, $r = 13.9$ and $r = 16$ for $L^2 = 14$, $L^2 = 16$, $L^2 = 18$ and $L^2 = 20$, respectively. As we know stable circular orbits corresponds to the minimum of the

effective potential while unstable orbits corresponds to the maximum of effective potential. We have stable circular orbits at $r = 9.1$, $r = 11.5$, $r = 13.5$ and unstable orbits at $r = 5.2$, $r = 4.6$, $r = 4.4$ for $L^2 = 16$, $L^2 = 18$ and $L^2 = 20$, respectively in figure 3.13 where $\alpha = 0.1$. In figure 3.14 and 3.15 there is no unstable circular orbits for the values of angular momentum used in figure 3.12 and graph becomes asymptotically constant. Hence, there are stable and unstable circular orbit for massive particles in the presence of string cloud parameter but there would be different situations for different values of string cloud parameter and angular momentum. It is concluded that the unstable circular orbits for massive particles exists for larger values of angular momentum L and smaller values of string cloud parameter α .

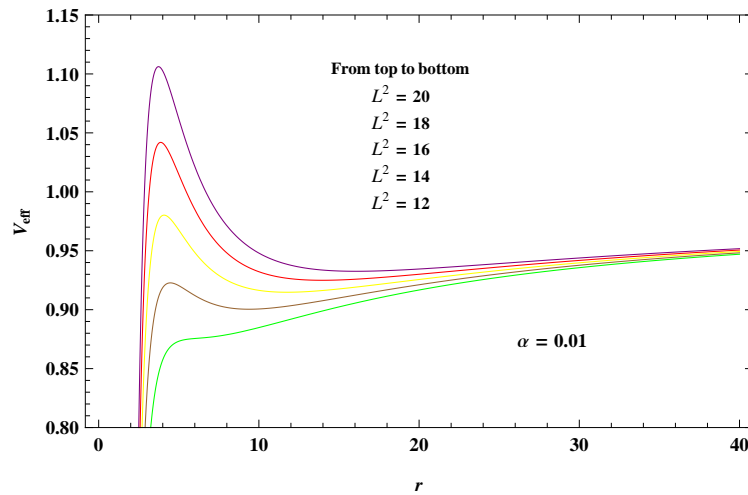


Figure 3.12: Effective potential for massive particles when $\alpha = 0.01$

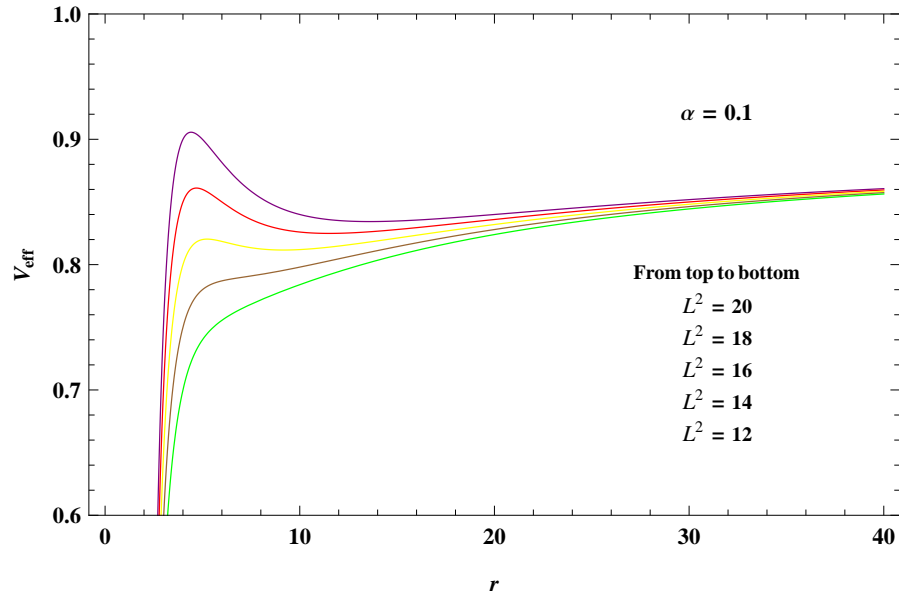


Figure 3.13: Effective potential for massive particles when $\alpha = 0.1$

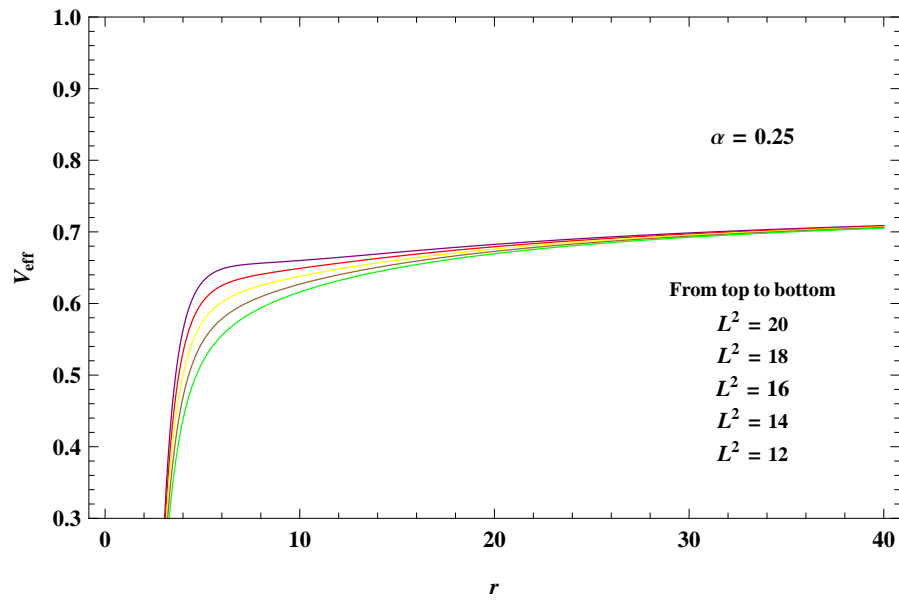


Figure 3.14: Effective potential for massive particles when $\alpha = 0.25$

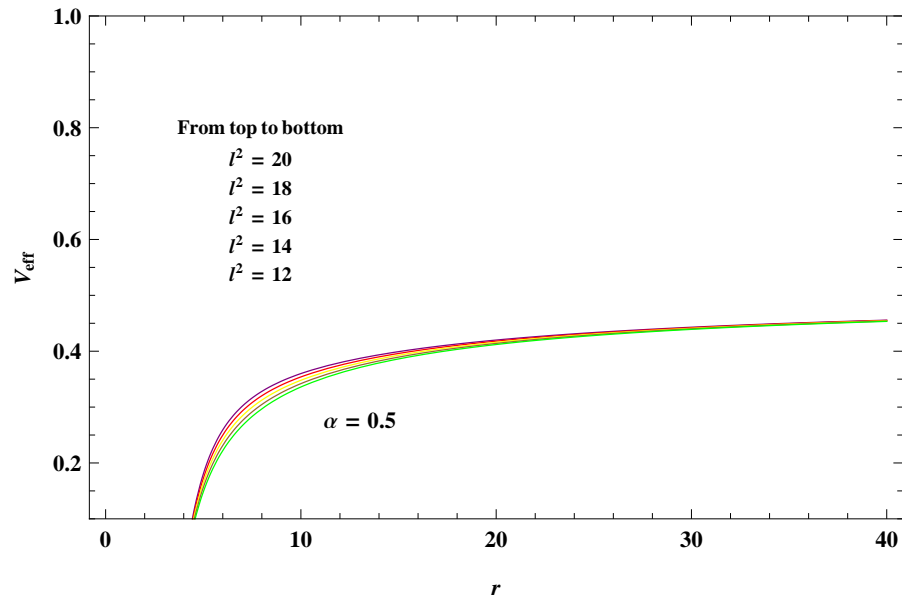


Figure 3.15: Effective potential for massive particles when $\alpha = 0.5$

Chapter 4

Summary and Discussion

In this dissertation we have studied trajectories of the timelike and null geodesics for radial and circular motion in the vicinity of the Schwarzschild black hole with string cloud background.

In the first chapter, basics of general relativity are studied. The derivation of EFEs in the presence of matter is given in the same chapter. Riemann tensor, stress-energy tensor and few features of black holes are also discussed there.

Second chapter is a review to the study of the discovery of constant radial force acted on pioneer spacecraft launched in 1972/73 [26]. Although the physical source of this force is still not known. There we reviewed the geodesics in the Grumiller spacetime. Where the effect of Rindler acceleration parameter on the trajectories of the timelike and null geodesics in Grumiller spacetime is compared with the Schwarzschild case. It was found that with the increasing value of Rindler parameter the effective potential also increases and particle

moves quickly towards the horizon, compared to the Schwarzschild case. It was seen that radial motion in the presence of Rindler parameter is bounded and there is no stable circular orbit for photons but, for the massive particle the stable circular orbits exist. It is noticed that radius of circular orbit of photons become smaller as Rindler parameter increases. Hence, Rindler parameter confine the geodesics. Rindler parameter does not allow the particle to escape to infinity.

In third chapter we have considered static spherically symmetric non vacuum solution in the presence of string cloud where α was the string cloud parameter. Therefore the particle was under the influence of both gravitational and string cloud parameter forces. We have obtained equations of motion by using Lagrangian formalism. It was found that in the presence of string cloud parameter the horizon was larger than the Schwarzschild horizon, as α approaches to unity radius of the horizon approaches to infinity. Effective potential was calculated and, it was observed that the effective potential decreases with the increase in string cloud parameter. It was observed that when string cloud parameter approaches to zero this leads to Schwarzschild case. Behavior of the particle with respect to time (proper/coordinate) in the presence of string cloud parameter was also investigated.

It was observed that for larger value of the string cloud parameter the circular orbit of photon has larger radius. Hence, as α increases the particle can more easily escape to infinity compared to the Schwarzschild case. We have also discussed the stability of circular orbits for photon and massive particles. It was found that there is no stable circular orbit for photons but for massive particles there are stable orbits as well as unstable circular orbits, depending on the values of angular momentum and string cloud parameter.

Bibliography

- [1] A. Qadir, *Relativity: Introduction to the Special Theory* (World Scientific, Singapore, 1989).
- [2] L. Amendola, S. Tsujikawa, *Dark Energy: Theory and Observation*, (Cambridge University Press, 2010).
- [3] K. Schwarzschild, Sitzungsberichte der Königlich Preußischen Akademie der Wissenschaften (Berlin), **1**, 189 (1916).
- [4] H. Stephani, D. Kramer, M. A. H. MacCallum, C. Hoenselaers, E. Herlt, *Exact Solutions of Einstein's Field Equations*, (Cambridge University Press, 2003).
- [5] H. Reissner, Annalen der Physik, **355**, 106 (1916).
- [6] G. Nordström, Koninklijke Nederlandse Akademie Van Wetenschappen Phys. Sci. B, **20**, 1238 (1918).
- [7] R. P. Kerr, Phys. Rev. Lett., **11**, 237 (1963).
- [8] E. Newman, E. Couch, K. Chinnapared, A. Exton, A. Prakash, R. Torrence, Math. Phys., **6**, 918 (1918).
- [9] M. P. Hobson, G. P. Efstathiou and A. N. Lasenby, *General Relativity: An Introduction for Physicist*, (Cambridge University Press, 2006).

- [10] V. P. Frolov, I. D. Novikov, *Black Hole Physics, Basic Concepts and New Developments*, (Springer, 1998).
- [11] V. Frolov, H. Falcke, *The Galactic Black Hole*, (IOP Press, 2003).
- [12] W. Israel, *Nature*, **209**, 66 (1966).
- [13] R. O. Hansen, *Astrophysical Journal*, **170**, 557 (1971).
- [14] S. Capozziello, A. Foeoli, G. Lambiase, G. Papini, G. Scarpetta, *Phys. Lett. A*, **268**, 247 (2000).
- [15] E. Honig, K. Lake, R. C. Roeder, *Phys. Rev. D*, **10**, 3155 (1974).
- [16] G. Denardo, R. Ruffini, *Phys. Lett. B*, **45**, 259 (1973).
- [17] N. Dadhich, P. P. Kale, *Pramana*, **9**, 71 (1977).
- [18] A. J. Armenti, *Il Nuovo Cimento B*, **25**, 442 (1975).
- [19] F. Felice, *Il Nuovo Cimento B*, **57**, 351 (1968).
- [20] F. Felice, M. Calvani, *Il Nuovo Cimento B*, **10**, 447 (1972).
- [21] Z. K. Kurmakaev, *Soviet Astronomy*, **18**, 110 (1974).
- [22] T. M. Helliwell, A. J. Mallinckrodt, *Phys. Rev. D*, **12**, 2993 (1975).
- [23] N. Dadhich, P. P. Kale, *Math. Phys.*, **18**, 1727 (1977).
- [24] Z. Stuchlik, *Bulletin of the Astronomical institutes of Czechoslovakia*, **32**, 366 (1981).
- [25] Z. Stuchlik, S. Hledik, *Class. Quantum. Grav.*, **17**, 4541 (2000).
- [26] M. Halilsoy, O. Gurtug, S. H. Mazharimousavi, *Gen. Relativ. Grav.*, **45**, 2363 (2013).

- [27] S. M. Carroll, *Spacetime and Geometry* (University of Chicago, 2004).
- [28] A. Qadir, *General Theory of Relativity* (Unpublished Lecture Notes).
- [29] S. Chandrasekhar, *The Mathematical Theory of Black Holes* (Oxford University Press, 1983).
- [30] O. Gron and S. Hervik, *Einstein's General Theory of Relativity* (Springer, 2007).
- [31] S. Carloni, D. Grumiller, F. Preis, Phys. Rev. D, **83**, 124024 (2011).
- [32] E. Groen, *Cosmic Strings* (Master's Thesis, University of Amsterdam, 2009).
- [33] I. Yavuz, I. Yilmaz, H. Baysal, Phys. Rev. D, **20** 45 (2008).
- [34] P. S. Letelier, Phys. Rev. D, **20**, 1294 (1979).
- [35] A. Ganguly, S. G. Ghosh, S. D. Maharaj, Phys. Rev. D, **90**, 064037 (2014).
- [36] E. Teo, Gen. Relat. Grav. **35**, 1909 (2003).
- [37] S. Hussain, I. Hussain, M. Jamil, Eur. Phys. J. C, **74**, 3210 (2014).
- [38] J. Pachner, Phys. Rev. Lett. A, **1**, 281 (1971).
- [39] R. Geroch, Annals of Physics, **48**, 526 (1968).
- [40] P. S. Letelier, Phys. Rev. D, **28**, 2414 (1983).
- [41] A. Strominger and C. Vafa, Phys. Lett. B, **379**, 99 (1996).
- [42] S. H. Mazharimousavi, M. Halilsoy, Phys. Lett. A, **28**, 1350073 (2013).
- [43] D. Grumiller, F. Phys. D, **20**, 2761 (2011).
- [44] D. Grumiller, Phys. Rev. Lett., **105**, 211303 (2010).

- [45] P. S. Letelier, Phys. Rev. D, **15**, 1055 (1977).
- [46] L. Susskind, Phys. Rev. D, **49**, 6606 (1994).
- [47] P. S. Letelier, Phys. Rev. D, **28**, 2414 (1983).
- [48] A. Vilenkin, Phys. Rev. D, **24**, 2082 (1981).
- [49] B. F. Schutz, *A First Course in General Relativity* (Cambridge University Press, 1985).
- [50] A. M. Al Zahrani, V. P. Frolov, and A. A. Shoom, Phys. Rev. D, **87**, 084043 (2013).
- [51] B. Punshly, *Black Hole Gravitohydrodynamics* (Springer, 2001).
- [52] L. D. Landau and E. M. Lifshitz, *The Classical Theory of Fields* (Oxford University Press, 1975).